MONITORING BÜLBÜLDERESİ AND BAKACAK LANDSLIDES WITH PHOTOGRAMMETRIC TECHNIQUES

A THESIS SUBMITTED TO
THE GRADUATE SCHOOL OF NATURAL AND APPLIED SCIENCES
OF
MIDDLE EAST TECHNICAL UNIVERSITY

BY

BÜKAY MURATOĞLU

IN PARTIAL FULFILLMENT OF THE REQUIREMENTS
FOR
THE DEGREE OF MASTER OF SCIENCE
IN
GEOLOGICAL ENGINEERING

MAY 2009

Approval of the thesis:

MONITORING BÜLBÜLDERESİ AND BAKACAK LANDSLIDES WITH PHOTOGRAMMETRIC TECHNIQUES

submitted by **BÜKAY MURATOĞLU** in partial fulfillment of the requirements for the degree of **Master of Science in Geological Engineering Department, Middle East Technical University** by,

Prof. Dr. Canan Özgen _____
Dean, Graduate School of **Natural and Applied Sciences**

Prof. Dr. M. Zeki Çamur _____
Head of Department, **Geological Engineering**

Assoc. Prof. Dr. M. Lütfi Süzen _____
Supervisor, **Geological Engineering Dept., METU**

Examining Committee Members:

Prof. Dr. Vedat Doyuran _____
Geological Engineering Dept., METU

Assoc. Prof. Dr. M. Lütfi Süzen _____
Geological Engineering Dept., METU

Prof. Dr. Tamer Topal _____
Geological Engineering Dept., METU

Assoc. Prof. Dr. Bora Rojay _____
Geological Engineering Dept., METU

Assoc. Prof. Dr. Murat Ercanoğlu _____
Geological Engineering Dept., Hacettepe University

Date: 13.05.2009

I hereby declare that all information in this document has been obtained and presented in accordance with academic rules and ethical conduct. I also declare that, as required by these rules and conduct, I have fully cited and referenced all material and results that are not original to this work.

Name, Last Name: Bükay Muratoğlu

Signature:

ABSTRACT

MONITORING BÜLBÜLDERESİ AND BAKACAK LANDSLIDES WITH PHOTOGRAMMETRIC TECHNIQUES

Muratoğlu, Bükay

M. Sc., Department of Geological Engineering

Supervisor: Assoc. Prof. Dr. M. Lütfi Süzen

May 2009, 87 pages

Every year, thousands of people all over the world are loosing their lives in natural disasters. As a second most widespread hazard, landslides are still a disaster problem for Turkey. The long-term monitoring studies of instability phenomena have a paramount importance for Turkey to reduce its both direct and indirect effects.

The objective of this thesis is to monitor the activity of the Bülbülderesi and Bakacak landslides in Asarsuyu Catchment for 42 years period by the digital aerial photogrammetric techniques while evaluating the possible use of archive aerial photography in such analysis.

To achieve the purpose of the study an orthophoto map was generated by aerial photographs belonging to 1994 year. The orthophoto map was utilized as a base map for aerial photo interpretation of different sets of aerial photographs corresponding to 1952, 1972, 1984 and 1994 years. As a result of this, 4 landslide activity maps are obtained. In addition, the characteristics of these landslides are analyzed by utilizing digital elevation model (DEM) created from stereo photographs of 1994.

As a result of the study, no considerable variation is detected in the position of main boundaries of Bülbülderesi and Bakacak landslides except some minor differences. However, within the landslides many topographical changes were observed between 1952 and 1994 period. Based on the profiles from toe to crest of the Bülbülderesi landslide, the approximate length was measured as 4773m whereas the approximate width was about 2614m. The areal extent was calculated as ~12km^2 having an approximate slope gradient ranging between 10-15° with local variations. On the other hand, the approximate length of Bakacak landslide was 4420m and the approximate width was 832m from toe to crest with an area of ~4km^2 and with an approximate slope angle 9-14°.

Keywords: Düzce, Bolu Mountain, Landslide, Digital photogrammetry, Orthophoto map

ÖZ

BÜLBÜLDERESİ VE BAKACAK HEYELANLARININ FOTOGRAMETRİ TEKNİKLERİ İLE İZLENMESİ

Muratoğlu, Bükay

Yüksek Lisans, Jeoloji Mühendisliği Bölümü

Tez Yöneticisi: Doç. Dr. M. Lütfi Süzen

Mayıs 2009, 87 sayfa

Her yıl, tüm dünyada doğal afetler yüzünden binlerce insan hayatını kaybetmektedir. En yaygın ikinci tehlike olarak heyelanlar Türkiye için hala bir afet sorunudur. Uzun süreli izleme çalışmaları duraysızlık olgusunun doğrudan ve dolaylı etkilerini azaltmak amacıyla Türkiye için fevkalade önem taşımaktadır.

Bu tezin amacı, Asarsuyu Havzası'ndaki Bülbülderesi ve Bakacak heyelanlarının 42 yıllık zaman dilimi içerisindeki etkinliğini arşiv hava fotoğrafları ile tespit ederken, aynı zamanda bu arşiv fotoğraflarının sayısal fotogrametrik değerlendirmeler ile kullanımını incelemektir.

Çalışmanın amacına ulaşmak için 1994 yılına ait hava fotoğraflarıyla bir ortofoto harita üretilmiştir. Ortofoto harita 1952, 1972, 1984 ve 1994 yıllarına ilişkin hava fotoğraflarının yorumlanmasında altlık harita olarak kullanılmıştır. Bunun sonucunda, 4 heyelan etkinlik haritası elde edilmiştir. Ayrıca, 1994'e ait stereo fotoğraflardan oluşturulan sayısal yükseklik modeli (SYM) kullanılarak heyelanların özellikleri analiz edilmiştir.

Bu çalışmanın sonucu olarak, bazı küçük farklılıklar dışında Bülbülderesi ve Bakacak heyelanlarının ana sınırlarının konumlarında önemli bir değişiklik saptanmamıştır. Ancak, 1952 ve 1994 arasındaki dönemde heyelanlar içinde birçok topografik değişiklik gözlenmiştir. Topuktan taca kadar olan profillere göre Bülbülderesi heyelanının yaklaşık uzunluğu 4773m yaklaşık genişliği ise 2614m olarak ölçülmüştür. Alanı ~12km^2, yerel değişikliklerle yamaç eğimi 10-15° olarak ölçülmüştür. Diğer taraftan, ~ 4km^2 alanı ve 9-14°lik yaklaşık eğim açısıyla topuktan taca Bakacak heyelanının yaklaşık uzunluğu 4420m ve yaklaşık genişliği 832m'dir.

Anahtar Kelimeler: Düzce, Bolu Dağı, Heyelan, Dijital fotogrametri, Ortofoto harita

To my dearest family and my beloved spouse

ACKNOWLEDGEMENTS

I would like to express my gratitude to my supervisor Assoc. Prof. Dr. M. Lütfi SÜZEN for his wisdom, clear guidance, critical vision, encouragements and endless support in every stage of this thesis. I feel really lucky to have a chance to work with him.

I would like to thank Assoc. Prof. Dr. Bora ROJAY for his precious scientific support. His valuable advices about the aerial photo interpretation process were very useful for me.

I am grateful to Alaattin MURATOĞLU for giving the opportunity to do this research and as all stages of this study are carried out with his facilities.

I would like to thank Ahmet BERK for his scientific support during this study. His valuable advices about photogrammetry were very useful for me.

I would like to express my thanks to Emine MURATOĞLU for her great motivation and endless encouragements.

I would like to thank also to Deniz GERÇEK for her valuable helps when I was in trouble with TNTMIPS.

I would like to thank to my dear friend Hilal SEVİNDİK for her guidance, motivation and encouragement in those hard working days.

I am grateful to Hayriye ÇAKMAK for her motivation and contributions for the improvement of this study. I would like to thank Selen ESMERAY for her help while preparing the format of this thesis. I would also want to thank to my friend Göktan İMAMOĞLU for technical support and being my personal Photoshop expert.

I would like to express my gratitude to my parents Oya & Tanzer SARDOĞAN and my brother Berkay SARDOĞAN for their endless love, continuous motivation, encouragements and understanding during my study. I would like to thank my beloved grandparents Müzehher & Orhan AKPULAT and Nimet ÖZKAYMAK for their endless love.

At last but definitely not least, I would like to show my very special thanks to my Cem for his unbelievable patience, unlimited motivation, endless love and clemency which I will need forever. He always believed me more than I do. Without the support of him, this study would not have been accomplished.

TABLE OF CONTENTS

LIST OF TABLES

TABLES

LIST OF FIGURES

FIGURES

CHAPTER 1

INTRODUCTION

Since the start of history natural disasters have menaced mankind and the world history has been shaped by them. As a result of this, millions of people have lost and will be loosing their lives all over the world.

Natural disasters are one of the most destructive events which are suddenly occurring, unavoidable, uncontrolled and causing loss of life and great damage to property. In other words, as Süzen (2002) stated that “disasters are natural hazard events in which a natural phenomenon or a combination of natural phenomena such as earthquakes, mass movements, floods, volcanic eruptions, tsunamis etc., can cause many loss of lives and damage to the property”.

According to Centre for Research on the Epidemiology of Disasters (CRED), natural disasters have been aggregated in three main categories; geophysical, biological, hydro-meteorological disasters. Furthermore, hydro-meteorological disasters are divided into three subgroups which are climatological (droughts, extreme temperatures and wildfires), hydrological (floods and wet mass movements) and meteorological disasters (typhoons, hurricanes, cyclones, storms, winter storms, tropical storms, tornadoes). On the other hand, geophysical disasters include earthquakes, volcanic eruptions and dry mass movements whereas biological disasters consist of epidemics, insect infestations and animal attacks (Scheuren et al., 2008).

In our country, due to its geological, seismic, topographical and climatic characteristics and combination of them provide a setting for many types of

natural disasters. Not only as a main disaster earthquake, but also mass movements and floods can be seen frequently in our country.

When the risk profile of Turkey is analyzed it is obviously seen that Turkey has many geological disadvantages due to lying more than 95% of the country in one of the most active earthquake and landslide regions in the world (Okay, 2005).

To emphasize the dramatic picture of Turkey based on the Emergency Events Database (EMDAT), the statistical information about the number of death, injured and affected people according to some types of natural hazards seen in Turkey is stated on Table1.1 (URL 1). Since the beginning of the 20th century about 91.500 people have lost their lives, about 94.000 people have been injured and about 9.000.000 people have been affected due to all natural disasters. The estimated damaged cost is around $25.000.000.000. It should also be noted that these numbers are somewhat underestimated especially in events rather than earthquakes as alerts of individual small events might not always reach to EMDAT to be considered.

Table 1.1. Number of casualties, injured and affected people due to some natural hazards occurred in Turkey (Emergency Events Database, 2009-URL1).

TYPES OF NATURAL HAZARDS	NUMBER OF CASUALTIES	NUMBER OF PEOPLE INJURED	NUMBER OF PEOPLE AFFECTED
Earthquakes	88.538	92.866	6.874.596
Landslides	665	254	14.344
Floods	1.274	180	1.743.386
Storms	100	139	13.639
Extreme Temperatures	100	450	8.450
TOTAL	**90.677**	**93.889**	**8.654.415**

Compared to previous years, there is an increasing trend in hydro-meteorological disasters across the world. Supporting that, reported hydrological

disasters in recent decades have increased by 7.4% per year, on average. Moreover, between the years 2000 to 2007, occurrence and impact of hydrological disasters have an average annual growth rate of 8.4% (Scheuren et al., 2008).

As the second most widely seen natural hazard, landslides are still disastrous for Turkey. The statistics claimed by Okay (2005) informed that 25% of country area is exposed to landslide hazard and 11% of total population is located in landslide areas. Moreover, 16% of total disaster losses are due to landslides. Some triggering factors that cause mass movements in Turkey are using slopes for agricultural purposes, natural vegetation removal, deforestation activities, inappropriate interaction of mankind with slopes, geological properties, earthquake and intense rainfall.

Unfortunately, landslides occur in all 81 provinces of our country. Nevertheless, particularly the Black Sea region is known as one of the most landslide-prone region in Turkey. According to Turkish Chamber of Geological Engineers (2006), in 1926 Of-Sürmene landslide 146 people lost their lives and 2211 buildings collapsed. As a result of 1985 West Black Sea landslides occurred in Zonguldak, Kastamonu and Sinop, 1684 residential estates were affected. In 1988, not only 64 people dead but also property was greatly damaged after 1988 Çatak landslide. After 1990 Trabzon, Giresun and Gümüşhane landslides, 65 people lost their lives and property had been enormously damaged. Furthermore, Senirkent landslide that occurred in 1995 caused 74 dead. Like 1998 Beşköy landslide, 2005 Koyulhisar-Kuzulu landslide caused great economic losses and casualties. The number of casualties of former was 50 and latter was 15. Therefore, all these examples prove that the long-term monitoring studies of slope instability phenomena have a paramount importance for countries to reduce its both direct and indirect effects.

1.1 PURPOSE AND SCOPE

In 1977 supported by United Nations Development Programme (UNDP) funds, with the participation of 13 European countries and 3 more countries having observer status, Trans-European Motorway (TEM) Project was started. In Turkey's borders started from Kapıkule then continued through the biggest industrial hub İstanbul to capital Ankara, Anatolian Highway is the major and crucial route between Europe and Asia. Besides being an alternative of D-100 road and its geopolitical significance, the Anatolian Highway reduces the average travel time between İstanbul and Ankara (Figure 1.1).

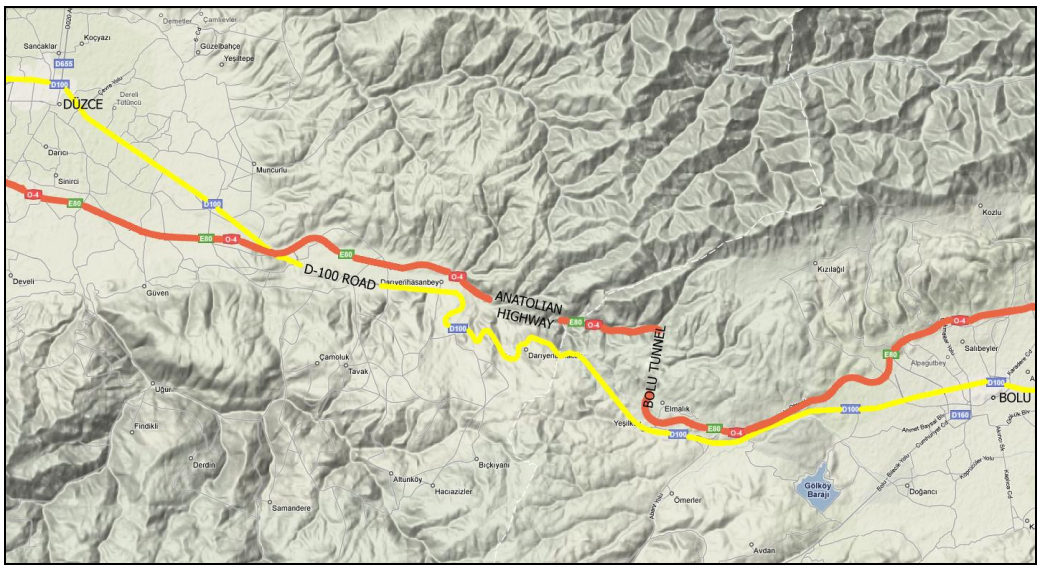

Figure 1.1. D-100 road and its alternative Anatolian Highway (TEM) that connect İstanbul to Ankara.

Being a part of the Anatolian Highway, Bolu Mountain Highway Pass is starting from Kaynaşlı, continuing in the east direction through Asarsuyu Valley, crossing Bolu Mountain and ending in Yumrukaya district on Gümüşova-Gerede route.

Apart from its geographical and economical significances, Bolu Mountain Highway Pass excites many people's interest due to encountered slope

instability problems during its construction. The Southeastern part of the Asarsuyu Catchment, especially Bolu Mountain Highway Pass is determined as having very high susceptibility to slope instabilities. The list of the reasons are: lack of lateral supports due to E-5 Highway cut slopes, proximity to active faults, extra vibration due to heavy traffic on E-5 Highway, the presence of flyschoidal units (Süzen, 2002; Süzen and Doyuran 2004a, b). Dalgıç (1998a) states that with a length of 4-5 km and width of 2-3 km. Bülbülderesi and 4-5 km length and 1.5 km. width Bakacak landslides are the largest landslides of the Asarsuyu Catchment. As toe of the Bülbülderesi landslide is passing close to a section of the Anatolian motorway where a 2.6 km long viaduct has been built, ensuring the stability of the slide is important for the long-term integrity of the structure.

The purpose of this thesis is to monitor the Bülbülderesi and Bakacak landslides for 42 years period to determine forthcoming behaviors of these slope movements in order to prevent potential life and property loss, while investigating the potential use and observing the limitations of stereo aerial photography in monitoring actions of large landslides.

1.2 GEOGRAPHICAL SETTING

The study area is located northwestern part of Turkey, between Düzce and Bolu cities, close to Kaynaşlı district (Figure 1.2). The area is covered by 1/25.000 scale topographic maps of quadrangles G26-b3, G26-b4, G26-c1 and G26-c2 of Adapazarı. The study area is bounded by the coordinates 4516000 N and 359000 E in the northwestern edge and 4510000 N and 365000 E in the southeastern edge in Universal Transverse Mercator (UTM) projection (Zone 36N, European Mean Datum 1950). The area is sited in Asarsuyu Catchment and covers approximately 36 km^2.

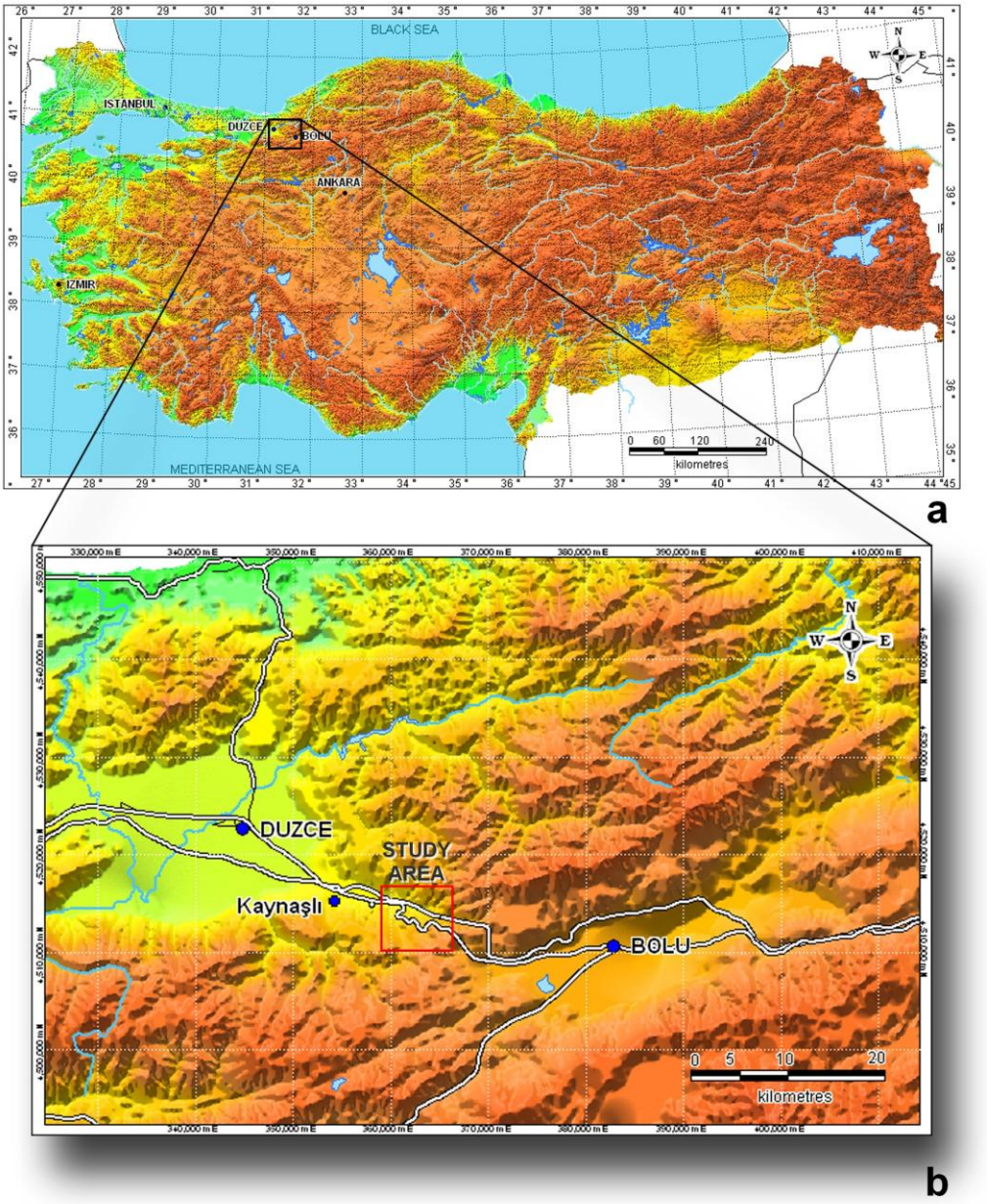

Figure 1.2. Location map of the study area. a) Color coded digital elevation model of Turkey, b) Location map of the study area within the Düzce-Bolu region.

1.3 LITERATURE SURVEY

Previous studies about landslide monitoring by means of digital photogrammetric techniques are presented in this section. Once the publications

and researches describing photogrammetric applications to landslides are taken into consideration, it is seen that the literature is quite scarce.

Monitoring landslide activity is of paramount importance for landslide studies. There are sophisticated tools available for monitoring geomorphological changes and landslide movements. Although traditional field-based geodetic, geotechnical and geophysical methods (Cencetti, et al., 2000, Yalçınkaya and Bayrak, 2001, Gürbüz et al., 2005) include inclinometers, piezometers, wire extensometers (Corominas et al., 2000), and land surveying devices (Franklin, 1984) that are necessary to acquire very precise information on specific locations in active landslides, these time consuming field procedures provide only point-based measurements and they do not give information about past movement episodes (Hervás et al., 2003). On the other hand, modern tools include Global Positioning Systems (Gili et al., 2000; Malet et al., 2002) and remote sensing methods (Hervás et al., 2003) such as satellite (Bajracharya, 2006; Tralli et al., 2005) and aerial imagery, Synthetic Aperture Radar (SAR) (Bovenga et al., 2006; Colesanti and Wasowski, 2006) and Light Detection and Ranging (LIDAR) (Adams and Chandler, 2002; Ager et al., 2004) enables to reconstitute both the recent and historical development of mass movements on different scales.

The development of photogrammetry started in 19th century after the invention of photography. The technical development of the photogrammetry has passed through the phases of plane table photogrammetry, analogue photogrammetry, analytical photogrammetry, and has entered the phase of digital photogrammetry since eighties due to improvements in computer technology (Konecny, 1985).

Photogrammetry, that is the measurement of shape, position, and dimension of objects on a surface from stereo photographs, is an effective and a powerful tool in geomorphological studies (Lane et al., 1993; Smith, 1996; Chandler, 1999). By using 3D stereo-photographs surface morphology can be accurately measured. The photographic archive provides an extensive source of

historical data allowing long-term analysis of surface changes, and has an important advantage over other monitoring systems (Lane et al., 1993; Lane et al., 1994). Combined with aerial photo interpretation, photogrammetric techniques are used to monitor slope movements.

At this point, Cheng (2000) examined the Tsau-Lin Big Landslide to reveal its condition and to compare the surface deformation before and after the 1999 Taiwan earthquake and suggests a method to integrate aerial photogrammetry, image processing and geographic information systems. After creating DTMs and orthophotos of the study area before and after the 1999 Taiwan earthquake by digital photogrammetric techniques, total area and volume of the landslide was estimated. Moreover, overtopping elevation and volume of the water storage of the upstream were calculated.

Mora et al. (2003) claimed that integration of GPS measurements and digital photogrammetry techniques become a powerful tool for movement monitoring including small displacements preceding the failure phase. In their study, the combination of kinematic GPS and digital photogrammetry was used to measure the surface displacements, rate of movement in the landslide body and to estimate the volume by generating precise DEMs of the Ca'di Malta landslide in Italy.

Karsli et al. (2004) studied the application of landslide activity maps created by digital photogrammetric techniques for evaluating the mass movement hazard in Ardeşen, Rize. The availability of multi-year aerial photo coverage integrated with field checks helped to assess the morphological changes and production landslide activity maps. As a result of this study, the sliding area was calculated and the quantity of the ground change in the landslide area was investigated by using profiles of the landslide.

Cardenal et al. (2006) carried out a study for the application of the digital photogrammetry in order to obtain very high quality information for landslide susceptibility maps and hazard analysis. They suggest a new methodology to

improve the prediction capacity of the landslide hazard maps by clearing some uncertainties due to poor resolution in the DEMs used in such maps. This methodology is based on the combined use of information related to landslide conditioning factors such as lithology, landcover, slope, meteorology, etc. and aerial photographs that were processed with digital photogrammetric techniques. Hence, a new high resolution DEM was obtained to be used for the susceptibility analysis.

Fernández et al. (2006) conducted a study by means of comparing digital photogrammetry techniques that are digitalization from ortophotographies (monoplotting), digitalization on aerial photographs and geometrical correction, translation to a topographical map and digitalization, and digital photogrammetric stereoplotting for the elaboration of landslides databases. The landslide scarp databases derived from different methodologies have been compared by displacement between significant points of scarps, the lengths of scarps and the fitness of scarps to a DTM. Finally, best results are obtained with the methodology of digital stereoplotting whose scarps database is well fitted to the DTM.

The multi-temporal monitoring of landslides in archaeological Incan site El Tambo, Ecuador was performed by Yugsi et al. (2006). In order to identify precisely the ground change in the study area, three sets of aerial photographs corresponding to different years were subjected to digital photogrammetry analysis. Then derived DTMs were used for orthophoto generation. 3D visualization and orthophoto interpretation enable to describe the slope instability processes that are occurring in the area and to correlate them with other key factors like type and level of erosion or type of material.

Mayuzumi and Ogawa (2006) studied the monitoring of several landslides by comparing two DEMs before and after the Niigata Chuetsu earthquake. These two DEMs were generated from aerial photographs by using digital photogrammetry techniques. To extract the ground change before and after the earthquake, the elevation values before the earthquake was subtracted from the

elevation values after the earthquake. In the differential image, the points of a minus value show decrease of the elevation values whereas the point of a plus value show increase of the elevation values by the earthquake. On the other hand, the points of a value 0 show changeless before and after the earthquake. Furthermore, the differential image was compared with 1/25.000 scale disaster map to identify the landslide points.

Another earthquake-triggered landslides developed along an active normal fault were investigated by Gallousi and Koukouvelas (2007) by means of digital photogrammetric analysis. The analysis of the landslides is based on a sequence of maps interpreted from both historical aerial photographs and direct field mapping. Geomorphic and volumetric evaluation of two landslides and drainage pattern were monitored by using generated DEM differences and orthophotos.

CHAPTER 2

GEOLOGY OF THE ASARSUYU CATCHMENT

2.1 REGIONAL GEOLOGY AND PREVIOUS STUDIES

The lithostratigraphical units of the study area are consist of various metamorphic, volcanic, sedimentary rock sequences represent a time interval from Paleozoic to Quaternary (Figure 2.1).

The main geographical features in the region are Asarsuyu River along southeast-northwest direction, Bolu Mountain and North Anatolian Fault Zone (NAFZ) extends along the length of the Asarsuyu Valley.

The Anatolian Highway that is the main artery between Ankara and İstanbul excites many scientists' interest due to the geographical significance of itself and the presence of the engineering problems during the construction of Bolu Tunnel. Several studies had been performed and focused on geology, engineering geology problems and tectonism of the region. Table 2.1 shows a brief summary of the accomplished studies in the research areas.

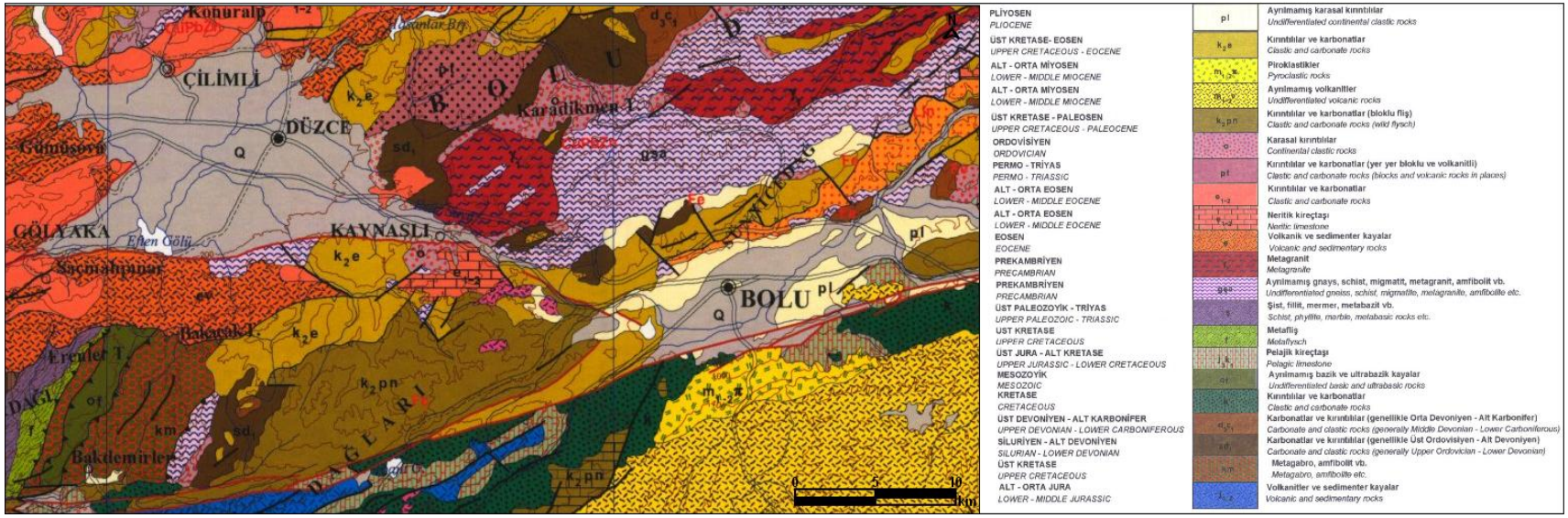

Figure 1.1. Regional geological map of the study area and its close vicinity (MTA, 2002).

Table 2.1. Previous studies of the study area (modified from Süzen, 2002)

	Researcher	Location	Studies
GEOLOGY	Blumenthal (1948)	Bolu Region	First definitions of tectonic units
	Ketin (1955)	Bolu Region	First sub-division of Paleozoic Massifs
	Uysallı (1959)	Bolu-Merkeşler	Geology of the region and Coal Resources
	Abdülselamoğlu (1959)	Mudurnu-Göynük	Definition of Paleozoic and Mesozoic formations
	Ketin (1967)	Bolu-Gerede-Mengen-Yığılca	Geology of the region (Paleozoic Units)
	Batum (1968)	Northern Slopes of Asarsuyu Valley	First defined the age of the conglomerates that overlie Bolu Massif as Silurian
	Orkan et al. (1977)	Bolu Mountain	Geology of the region
	Gözübol (1978)	Mudurnu-Dokurcun-Abant	Geology of the region
	Görmüş (1980)	Yığılca	Stratigraphy of the region
	Yılmaz et al. (1981)	Abant-Dokurcun	Evolution of tectonic units, relations of metamorphic rocks and the ophiolitic rocks
	Görmüş (1982a)	Yığılca	Stratigraphy of the region
	Görmüş (1982b)	Yığılca	Geologic evolution of the region
	Kaya (1982)	Ereğli-Yığılca-Bolu-Mengen	Stratigraphy of the region
	Kaya & Dizer (1981-1982a)	Mengen	Stratigraphy of coal resources
	Kaya & Dizer (1981-1982b)	North Bolu	Stratigraphy of Upper Cretaceous and Paleocene sequences
	Cerit (1983)	Mengen	Geology of the region
	Serdar & Demir (1983)	Bolu-Mengen-Abant	Geology of the region and petroleum resources
	Öztürk et al. (1984)	Abant-Yeniçağa	Stratigraphy of north and south of NAFZ
	Kaya et al. (1986)	Yığılca	Stratigraphy of Upper Cretaceous and Paleocene sequences
	Aydın et al. (1987)	Çamdağ-Sünnicedağ	Complete stratigraphic outline
	Cerit (1990)	Bolu Massif	Geology of the region
	Erendil et al. (1991)	Bolu Massif	Geology of the region
	Yalçın & Cerit (1991)	Bolu Massif	Mineralogy and geochemistry of clay minerals
	Koral et al. (1994)	Asarsuyu	Microfabric study in Paleozoic rocks
	Gedik & Alkaş (1996)	Bolu Region	Geology and Carbondioxide potential
	Sözen et al. (1996)	Düzce-Devrek	Geochemistry of the region
	Güler (1999)	Bakacak	Geological studies
	Ustaömer & Rogers (1999)	Bolu Massif	Geochemistry and evolution of the Bolu Massif

Table 2.1. (Continued)

	Özmen (2000)	Düzce-Bolu	Geology of the region
	Kazak (2004)	Bolu	Geology of southeast part of the Bolu Basin
	Karaçam (2005)	Bolu-Gökçesu	Investigation of reservoir geology of the units
ENGINEERING GEOLOGY	Canik (1980)	Bolu	Hydrogeology of the region
	Aktimur et al. (1983)	Bolu Region	Landuse pattern and NAFZ related problems
	Astaldi (1990)	Anatolian Motorway	Preliminary design of Gümüşova-Gerede stretch
	Dalgıç (1994 a,b)	Bolu Mountain Highway Pass	Engineering geology of Highway pass and Bolu Tunnel
	Dalgıç et al. (1995)	Asarsuyu	Stability and nature of the Yumrukaya landslide
	Dalgıç & Gözübol(1995)	Bolu Tunnel	Stability problems in tunnel
	Dalgıç (1997)	Bolu Tunnel	Lithology and the fracture pattern in the Bolu Tunnels
	Simşek & Dalgıç (1997)	Düzce	Consolidation properties of clays
	Aydan & Dalgıç (1998)	Bolu Tunnel	Prediction of deformation inside the Bolu Tunnel
	Dalgıç (1998,a)	Asarsuyu	Slope stability problems in the Asarsuyu valley
	Dalgıç (1998,b)	Asarsuyu	Selection of crushed rock quarries for the construction of the Anatolian Motorway
	Işın (1999)	Kaynaşlı-Elmalık	Geotechnical studies on Taşaltı landslide area
	Şentürk (1999)	Bolu Tunnel	Engineering geology and geotechnical characteristics of Bolu Tunnel
	Unterberger and Brandl (2000)	Bolu Tunnel	Deformations in the Bolu Tunnels after Düzce earthquake
	Aydan et al. (2000)	Düzce	Engineering geological, seismological and geotechnical aspects of Düzce earthquake
	Sucuoğlu et al. (2000)	Regional	Engineering report of the Marmara and Düzce earthquakes
	Süzen (2002)	Asarsuyu	Landslide Hazard Assessment by using GIS and Remote Sensing
	Aksu (2002)	Gümüşova-Gerede	Engineering geology studies
	Süzen and Doyuran (2004a)	Asarsuyu	Data driven bivariate landslide susceptibility assessment using GIS
	Süzen and Doyuran (2004b)	Asarsuyu	A comparison of the GIS based landslide susceptibility assessment methods multivariate versus bivariate

Table 2.1. (Continued)

	Özben (2003)	Bolu Tunnel	Engineering geology of Bolu Mountain Tunnel
	Yeşilnacar and Süzen (2006)	Asarsuyu	A land-cover classification for landslide susceptibilty mapping
	Pamuksuz (2007)	Bolu-Mengen	Engineering geology of Köprübaşı Dam
TECTONICS	Ketin (1969)	Regional	First definition of NAFZ
	Ambraseys(1970)	Regional	Characteristic features of NAFZ
	Tokay (1973)	Gerede-Ilgaz	Characteristics of NAFZ
	Gözübol (1978)	Mudurnu-Dokurcun-Abant	Structural properties of NAFZ
	Şengör & Canıtez (1982)	Regional	Characteristics and evolutionary model of NAFZ
	Öztürk et al. (1984)	Abant-Yeniçağa	Paleo and Neo-tectonic structures
	Cerit (1990)	Bolu Massif	Tectonic setting of the region
	Demirtaş (1993)	İğneciler-Dokurcun	Neotectonics and seismicity of NAFZ
	Nurlu (1993)	Bolu-Sapanca	Fault analysis by using remote sensing
	Barka and Erdik (1993)	Gümüşova-Gerede	Active Faults of Gümüşova-Gerede Highway
	Neugebauer (1994)	Abant	Closing-up structures, effects of bends in NAFZ
	Neugebauer (1995)	Adapazarı-Bolu	Structures and kinematics of NAFZ
	Şaroğlu et al. (1995)	Yeniçağa-Gerede-Eskipazar	Geology of the region and characteristics of NAFZ
	Neugebauer et al. (1997)	Abant-Sapanca	Seismic observations of the western NAFZ
	Demirtaş (2000)	Abant-Gerede	Paleoseismicity and neotectonics of NAFZ
	Akyüz et al. (2000)	Düzce	Slip distributions of Düzce Earthquake
	Taymaz (2000)	Gölcük-Sapanca-Düzce	Seismotectonics of Marmara region
	Özmen (2000)	Düzce-Bolu	Active faults and earthquakes of the region
	Özden et al. (2000)	Düzce	Düzce earthquake and tectonism of the region
	Aksu (2002)	Gümüşova-Gerede	Engineering geology and tectonism of the region
	Hitchcock et al. (2003)	Düzce	Late Holocene Earthquakes on the Eastern Düzce Fault and Implications
	Kazak (2004)	Bolu	Neotectonics of southeast part of the Bolu Basin
	Şengör et al. (2005)	Regional	Characteristics of NAF
	Pucci et al. (2007)	Düzce	The Düzce segment of NAF

2.2 GENERAL STRATIGRAPHY OF ASARSUYU CATCHMENT

In this study, for the description of the geological units in and around the Asarsuyu Catchment, the nomenclature proposed by Süzen (2002) is adopted. The geological map of the study area and the stratigraphic columnar section are shown in Figure 2.2 and Figure 2.3, respectively.

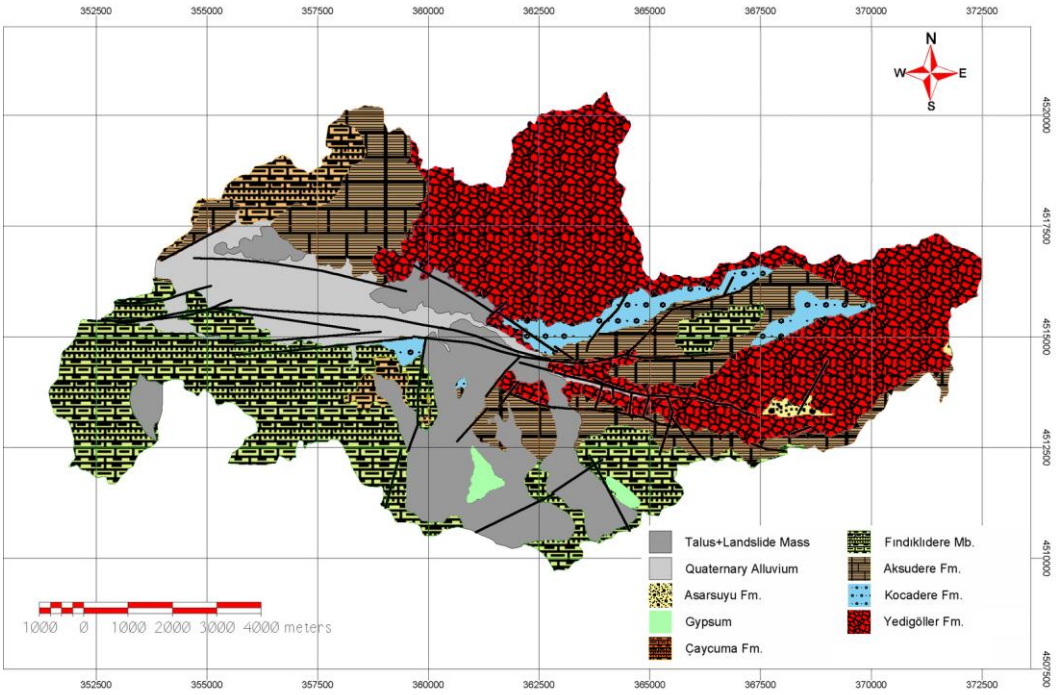

Figure 2.2. Geological map of the study area (Süzen, 2002).

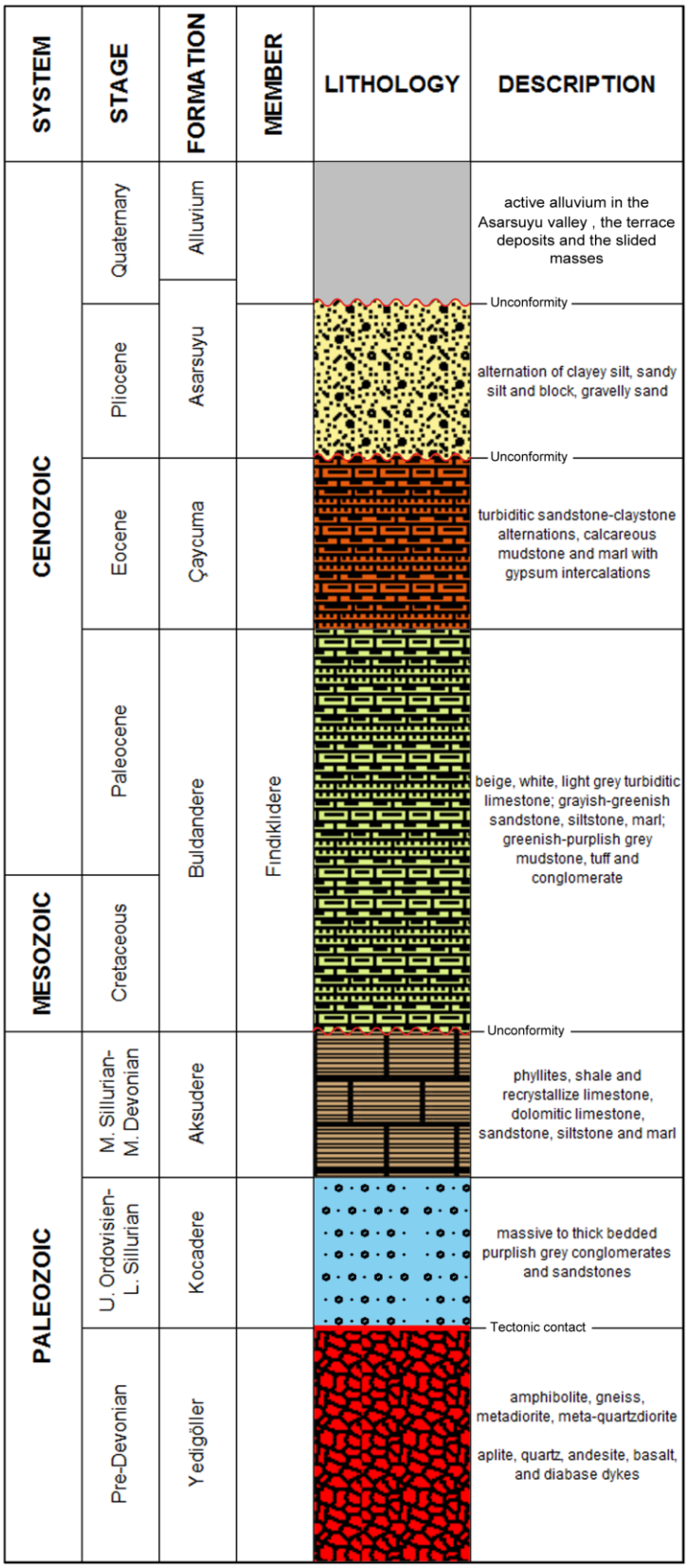

Figure 2.3. Generalized stratigraphic columnar section of the study area (Erendil et al., 1991; not to scale).

2.2.1 Yedigöller Formation

Yedigöller Formation is the local geologic basement and the core of the Bolu Massif. The formation comprises southwestern part of the Bolu Massif and is mainly composed of jointed and fractured amphibolite, gneiss (metagranite), metadiorite and meta-quartzdiorite and first named by Aydın et al. (1987). Yedigöller formation is overlain by Devonian İkizoluk Formation is composed of phyllite, slate and limestone with tectonic contact, which does not outcrop in the Asarsuyu catchment (Dalgıç, 1994a). Due to excessive cataclastic metamorphism, some of these lithologies turn into mylonitic rocks. Near fault zones, cataclastic deformation can be observed and thought to be related to tectonic events occurred in the region.

The age of the metamorphics are determined as Paleozoic by Blumenthal (1948). Ketin (1967) cited the age of the assemblage of amphibolite, gneiss and basic rock in Bolu-Gerede-Mengen-Yığılca region as Pre-Cambrian. Canik (1980) suggested that at the northeastern part of Bolu, Cambrian red sandstone overlies the metamorphic units such as gneiss, biotite, muscovite and albite. Therefore, like Canik (1980), Aydın et al. (1987) and Cerit (1990) concluded that the age of the formation should be Precambrian. On the other hand, Erendil et al. (1991) claimed that the age of the formation is Pre-Late Ordovician. As a result of these arguments, the age of the Yedigöller Formation is assigned as Pre-Devonian.

2.2.2 Kocadere Formation

Erendil et al. (1991) defined Kocadere Formation that is represented by massive to thick bedded purplish grey conglomerates and sandstones. Reddish brown mudstone-siltstone alternations (3mm-3cm) can be observed in sandstones. Conglomerates are poorly sorted, and their components are derived from underlying metamorphics, and magmatic rocks. Also, conglomerates are composed of granite, granodiorite, amphibolite, chlorite and quartz. The matrix

of greywacke consists of quartz fragments, chlorite and sericite. Moreover, the formation does not have any fossil content (Erendil et al., 1991).

Kocadere formation is overlain by Aksudere formation conformably. The equivalent of this formation is defined by Kaya (1973) as Kurtköy Formation of Ordovician age. The other equivalents of Kocadere formation are "Hamzafakılı sandstones" (Tokay, 1952), Işığandere Formation (Görmüş, 1982 a, b) and "purple arkoses and conglomerates" (Batum, 1968) with the age of Late Silurian. Canik (1980) determined the age of other equivalent Çukurviran Formation as Silurian. The age of Kocadere Formation is determined as Late Ordovician-Early Silurian (Erendil et al., 1991).

2.2.3 Aksudere Formation

The formation composed of phyllites, shale and recrystallized limestone, dolomitic limestone, sandstone, siltstone and marl that are easily eroded and represented by dark grey, beige, bluish-greenish grey and brown (Erendil et al., 1991).

The upper boundary is conformable with Kırdoruk Formation which is not observed in the study area. Görmüş (1982a) defined the equivalent of the lower facies of this formation as Kocadere formation that is determined as Early Devonian age. On the other hand, the equivalent of the upper facies defined as Middle Devonian Hacıyerdere Formation. Önalan (1981) stated that Silurian Gözdağ Formation and Late Silurian Dolayoba Formation are correlated with the lower facies of Aksudere formation. Kaya (1973) defined Aksudere formation equivalent with Kartal formation consist of mudstone-sandstone-limestone alteration characterized by dark grey, fine grained mudstone, yellowish-brownish fine grained, thin bedded sandstone and dark grey, sandy, thick laminated limestone. Dalgıç (1994a, b) grouped the Kocadere and Aksudere formations under İkizoluk formation consist of phyllitic rocks, slates and limestones and assigned an age of Devonian. Also he claimed that the İkizoluk Formation overlies Yedigöller Formation with a tectonic contact. The

age of the Aksudere Formation is assigned as Late Silurian to Early-Middle Devonian (Erendil et al., 1991).

2.2.4 Buldandere Formation

Erendil et al. (1991) described all of the Upper Cretaceous-Paleocene units that cover the Paleozoic Bolu Massif as Buldandere Formation that consists of marine sediments and volcanic-volcanoclastic units. The formation is separated into three units which are İspahlar, Fındıklıdere and Devretkaya members that overlie the Bolu Massif (Erendil et al., 1991). However, only Fındıklıdere member can be observed in the study area.

2.2.4.1 Fındıklıdere Member

The formation contains gradational layers of beige, white, light grey turbiditic limestone; grayish-greenish sandstone, siltstone, marl; greenish-purplish grey mudstone, tuff and conglomerate. The Çaycuma Formation overlies Fındıklıdere member conformably. Based on the fossil content the age of this formation is determined as Campanian – Ilerdian by Erendil et al. (1991). The equivalent of this formation is stated as Cretaceous Flysch (Abdülselamoğlu, 1959), Eocene Gökveren Formation (Gözübol, 1978 and Yılmaz et al., 1981), Upper Cretaceous/Paleocene Sarıkaya Formation (Görmüş, 1980), Campanian/Lower Paleocene Akveren Formation (Ketin and Gümüş, 1963; Gedik and Korkmaz, 1984; Aydın et al., 1987), Upper Cretaceous/Paleocene Fındıcak Formation (Dalgıç, 1994a, b).

2.2.5 Çaycuma Formation

The formation is composed of turbiditic sandstone-claystone alternations, calcareous mudstone and marl with gypsum intercalations and firstly named by Saner et al. (1979). The lower facies of this formation is represented by pyroclastic and volcanic rocks and named as Melendere Member that cannot be observed in the study area. The lower boundary of Çaycuma Formation is

conformable with Fındıklıdere Member. However, its upper boundary is unconformable with Asarsuyu Formation (Erendil et al., 1991).

Görmüş (1982) defined the equivalent of Çaycuma Formation as Alaptura Formation with an age of Middle Eocene. On the other hand, other similar unit is stated by Dalgıç (1994a, b) as Late Eocene Açma Member characterized by alternations of grey-beige argillaceous limestones, gypsums, calcareous mudstones and white-beige clayey gypsums. Based on the fossil records the age of the formation is assigned as Eocene by Erendil et al. (1991).

2.2.6 Asarsuyu Formation

The main lithologies of the formation are alternation of clayey silt, sandy silt and block, gravelly sand. Asarsuyu Formation is assigned an age of Quaternary and named by Dalgıç (1994a, b). Furthermore, he differentiated this formation from Quaternary Deposits. The upper boundary of the Asarsuyu Formation is unconformable with Quaternary alluvium.

The age of this formation is assigned by Abdülselamoğlu (1959), Gözübol (1978), Aydın et al. (1987) and Canik (1980) as Pliocene and is supported by fossil records. For the age of Plio-Quaternary is based on palynological data by Astaldi (1990).

2.2.7 Quaternary Deposits

The quaternary deposits are the youngest units in the study area and are categorized as slope debris, alluvial cone and alluvium by Dalgıç (1994a). According to Dalgıç and Şimşek (2002) these alluvium deposits are generally observed in the Asarsuyu Valley and are consist of rounded, subrounded, pebbly sand, blocky pebbly sand and blocky pebbles derived from weakly altered, intermediately soft-very compact amphibolite, metagranite.

2.3 TECTONIC SETTING OF ASARSUYU CATCHMENT

The study area is located at the western part of the Pontide Belt, within the North Anatolian Fault Zone. In addition to being the most prominent currently active right lateral strike-slip fault, NAF extends approximately 1500 km across northern Turkey (Şengör et al., 2005). Being within the NAFZ, Düzce-Bolu area is one of the most tectonically active regions represented in Figure 2.4 (URL 2).

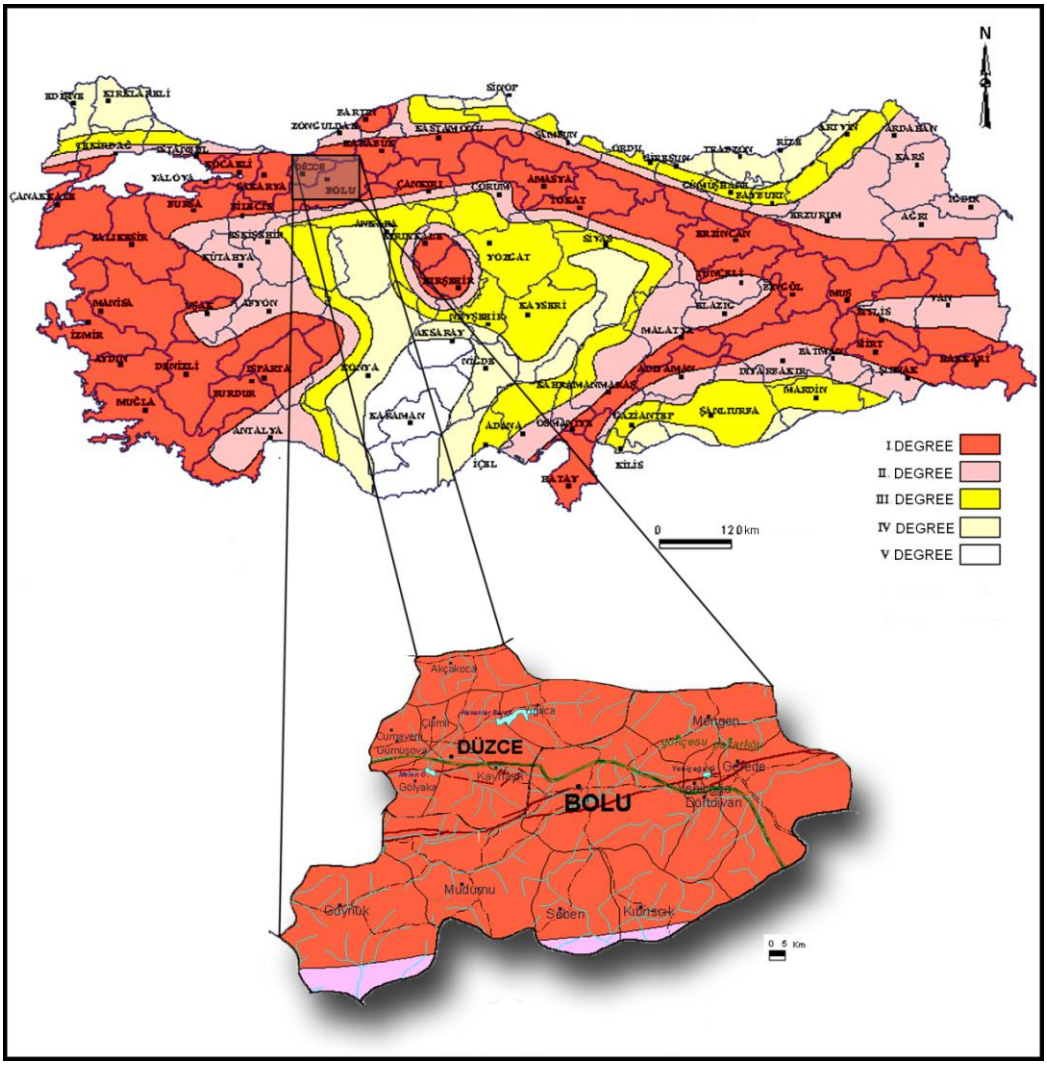

Figure 2.4. Earthquake zone map of Turkey and Düzce-Bolu region (General Directorate of Disaster Affairs, 1996-URL2)

Associated with NAF, Düzce, Bakacak and Elmalık are the active faults that control the tectonism of the region (Barka and Erdik, 1993; Hitchcock et al., 2003) are shown in Figure 2.5.

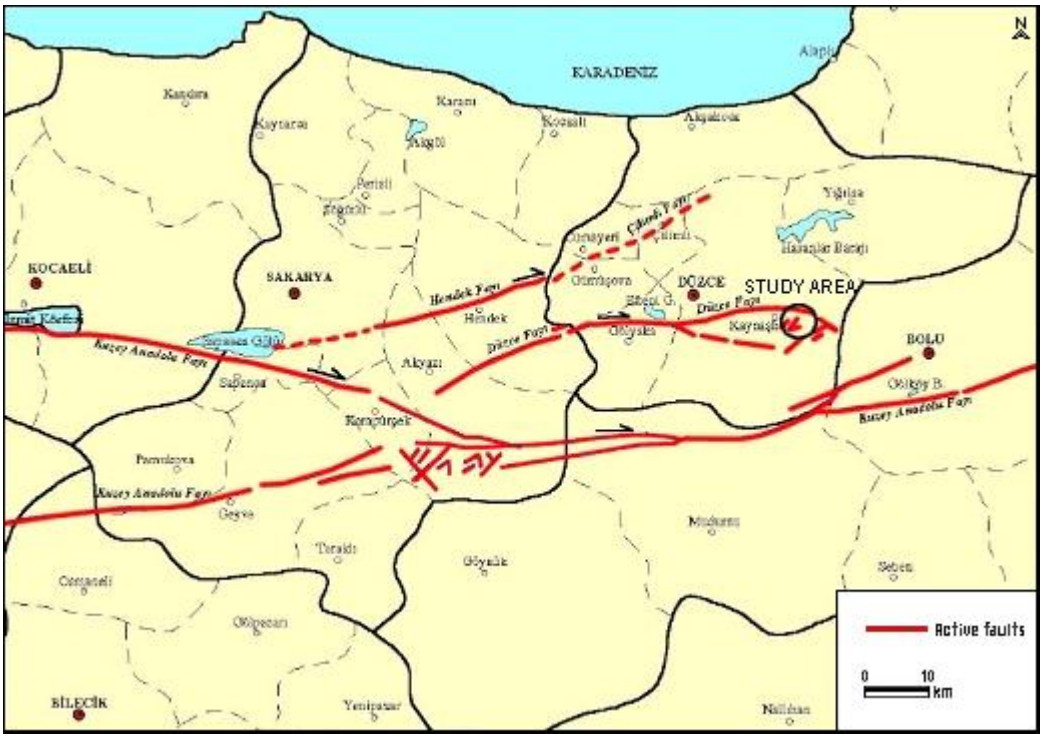

Figure 2.5. Map showing the active faults in Düzce-Bolu region (Özmen, 2000).

The Düzce fault appears in the east to join the single trace of the NAFZ via a right-releasing step-over formed by the WNW–ESE trending Bakacak and Elmalık faults (Pucci et al., 2007). The Düzce fault plays an important role in the deformation and morphological evolution of the area; its right lateral strike-slip motion formed the Düzce Basin (Şimsek and Dalgıç, 1997). Özden et al. (2000) states that this E-W trending fault extends from Akyazı in the west to Bolu Tunnel in the east, with a length of 75 km. Düzce fault is the northern branch of the NAF system and is the source of the 12 November 1999 earthquake (M=7.2). As a result of this earthquake, 40 km long surface rupture between Gölyaka and the Bolu Mountains was occurred, and some part of the Bolu Tunnel had been collapsed resulting in abandonment of collapsed part and

later the tunnel was re-routed. Being a 10-15 km long active strike slip fault, Bakacak fault extends southeastward from the Düzce fault to west of Bolu. On the other hand, Elmalık fault is a northwest-southeast trending fault that extends for a distance of about 15 km into the Bolu Basin. Based on the palaeoseismic trench data, these two faults are evidences of Holocene fault activities (Hitchcock et al., 2003).

When the seismicity of the study area and its vicinity is examined, it is detected that a total of 1425 earthquakes, of which 196 greater than 4 in magnitude have been recorded from January 1900 to March 2009. Particularly, 4 of them greater than 7 in magnitude listed chronologically as 26.05.1957 Abant (M=7.1), 22.07.1967 Mudurnu (M=7.2), 17.08.1999 Marmara (M=7.4) and 12.11.1999 Düzce (M=7.2) earthquakes. The locations of all earthquakes with their magnitudes occurred in the study area and its environs are shown in Figure 2.6 (URL 3).

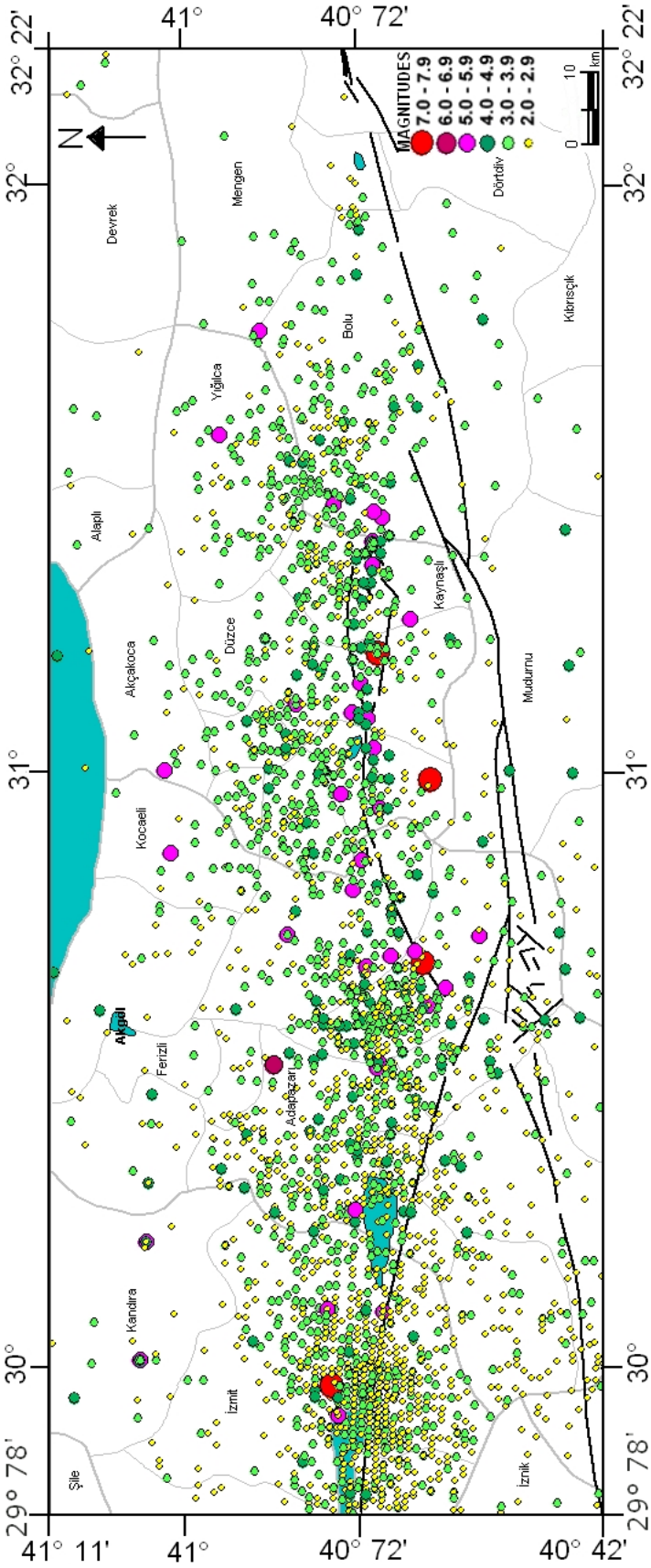

Figure 2.6. Epicenter locations with magnitudes of the study area and its environs (Sayısal Grafik, 2009-URL3).

CHAPTER 3

METHODOLOGY

In this section, the application of orthophoto map generation, DEM difference and aerial photo interpretation is explained in order to monitor Bülbülderesi and Bakacak landslides. The main steps of the process are displayed according to the flowchart diagram below (Figure 3.1).

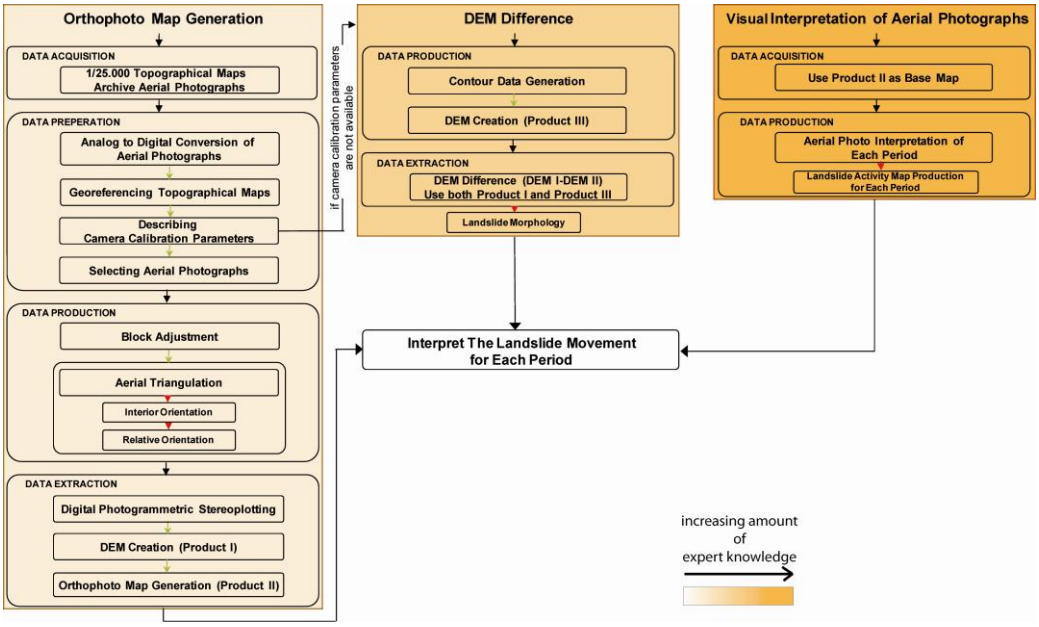

Figure 3.1. Flowchart for the applied methods.

3.1 ORTHOPHOTO MAP GENERATION

3.1.1 Data Acquisition

For the area under investigation 1/25.000 scale topographical maps corresponding to source dates of 1952, 1972 and 1994 years and 4 different sets of stereo black and white aerial photographs corresponding to 1952, 1972, 1984 and 1994 years are ensured from General Command of Mapping.

3.1.2 Data Preparation

The data preparation stage consists of analogue to digital conversion of aerial photographs, georeferencing topographical maps, describing camera calibration parameters and selecting aerial photographs for the analyses for the next stage.

3.1.2.1 Analog to Digital Conversion of Aerial Photographs

First of all, the aerial photographs have to be scanned to digital format before they can be used in digital photogrammetry applications. For the years 1952, 1972, 1984 and 1994, 4 sets of stereo pair photographs covering the study area were scanned by a desktop scanner at a resolution of 63 μm which corresponds to 400 dpi. The size of the photographs for 1952 is 17,5 x 17,5 cm and for 1972, 1984 and 1994 is 23 x 23 cm. Although the scale of 1952 photos denominated as 1/35.000 by General Command of Mapping, the scale of photos were calculated as 1/20.000. The ground resolution indicates the distance on the ground that's represented by a single pixel in the map was calculated as:

$$Ground\ resolution\ (m) = \frac{0{,}0254\ (m/inch)}{Map\ scale \times Screen\ resolution\ (dpi)} \tag{3.1}$$

The equation of flight height could be written in its simplest form as:

$$FH(m) = \frac{FL(m)}{MS} \tag{3.2}$$

where FH is flight height above terrain, FL is focal length of the camera and MS is map scale.

Table 3.1. The main characteristics of aerial photographs.

Year	Scale	Size (cm)	Ground Resolution (m)	Calculated Flight Height (m)	Focal Length of Camera (mm)
1952	1/20.000	17,5 x 17,5	1.26	4200	99.69
1972	1/25.000	23 x 23	1.58	4500	152.79
1984	1/15.000	23 x 23	0.95	3000	151.86
1994	1/35.000	23 x 23	2.21	6050	153.29

3.1.2.2 Georeferencing Topographical Maps

Corresponding to 1952, 1972, 1994 years, 1/25.000 digitized topographic maps in sheets G26-b3, G26-b4, G26-c1 and G26-c2 of Adapazarı were georeferenced by using at least four ground control points of the map grids. The coordinates were in ED50/UTM projection system zone 36. The root mean square errors of all these maps were calculated and presented on Table 3.2, Table 3.3 and Table 3.4. Although only four points are adequate for affine transformation, in some cases, especially in 1952's sheets many points were used for registration because of the deterioration in quality of the maps. According to technical specifications of topographic maps, General Command of Mapping (URL 4) claims that average accuracy of maps is 5m in horizontal and 2,5m in vertical.

Map sheets of 1952, 1972 and 1994 years were produced from aerial photographs of the same years by aerial photogrammetry technique. Then, these maps were revised and printed in different years (Table 3.2, Table 3.3 and Table 3.4). Each set of digital topographical maps covered the study area are presented on Figure 3.2, Figure 3.3 and Figure 3.4.

Table 3.2. Source, revised, printing dates and RMS error values of the topographic maps (1952 period).

Map Sheets	Source Date	Revised Date	Printing Date	RMS Errors (m)
G26-b3	1952	1955-1956	1959	1,96
G26-b4	1952	1955-1956	1959	1,65
G26-c1	1952	1955-1956	1960	4,12
G26-c2	1952	1957	1957	1,95

Table 3.3. Source, revised, printing dates and RMS error values of the topographic maps (1972 period).

Map Sheets	Source Date	Revised Date	Printing Date	RMS Errors (m)
G26-b3	1972	1983	1984	1,94
G26-b4	1972	1980	1981	1,72
G26-c1	1972	1973	1977	1,85
G26-c2	1972	1974	1977	1,87

Table 3.4. Source, revised, printing dates and RMS error values of the topographic maps (1994 period).

Map Sheets	Source Date	Revised Date	Printing Date	RMS Errors (m)
G26-b3	1994	1995	1997	0,96
G26-b4	1994	1995	1997	1,54
G26-c1	1994	1995	1997	1,24
G26-c2	1994	1995	1997	1,22

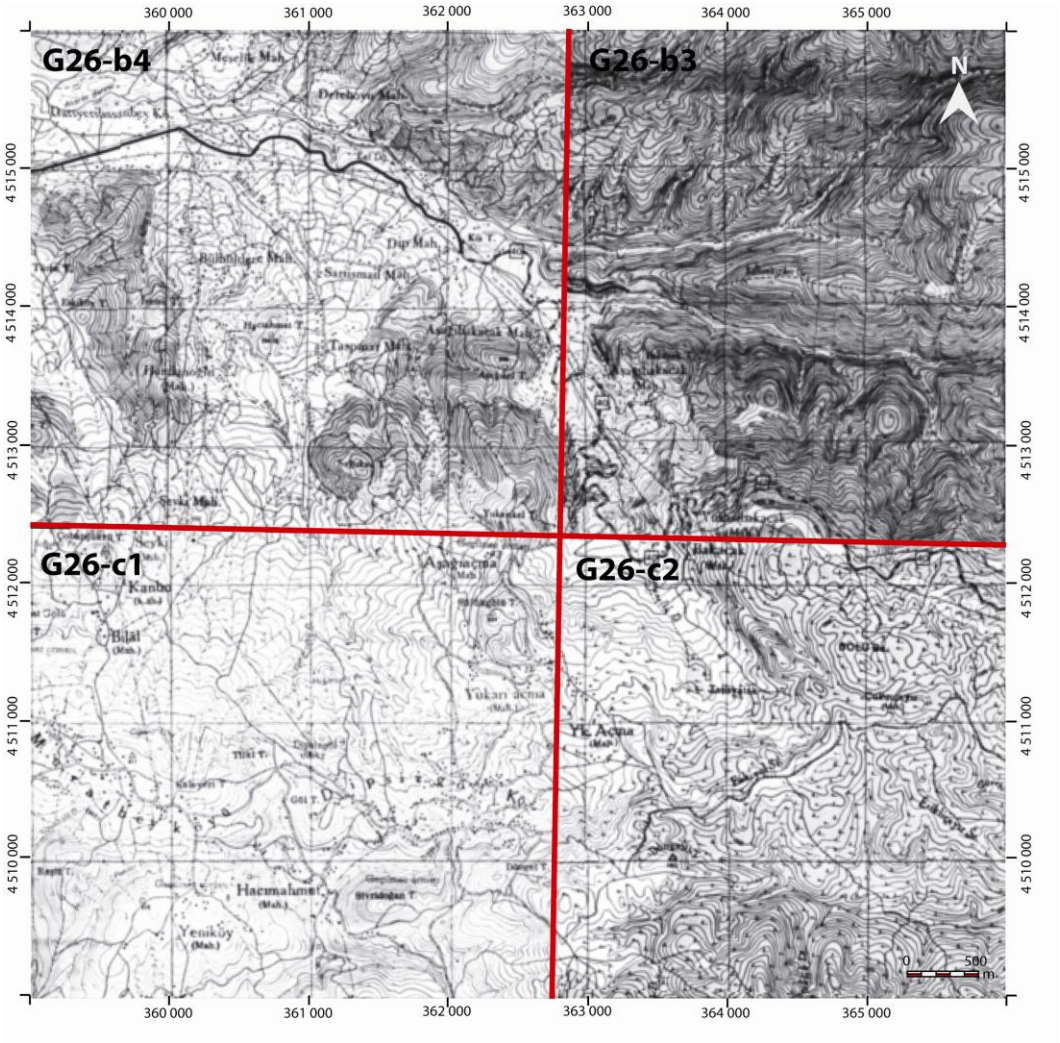

Figure 3.2. Topographic map of quadrangles G26-b3, G26-b4, G26-c1 and G26-c2 (1952 period).

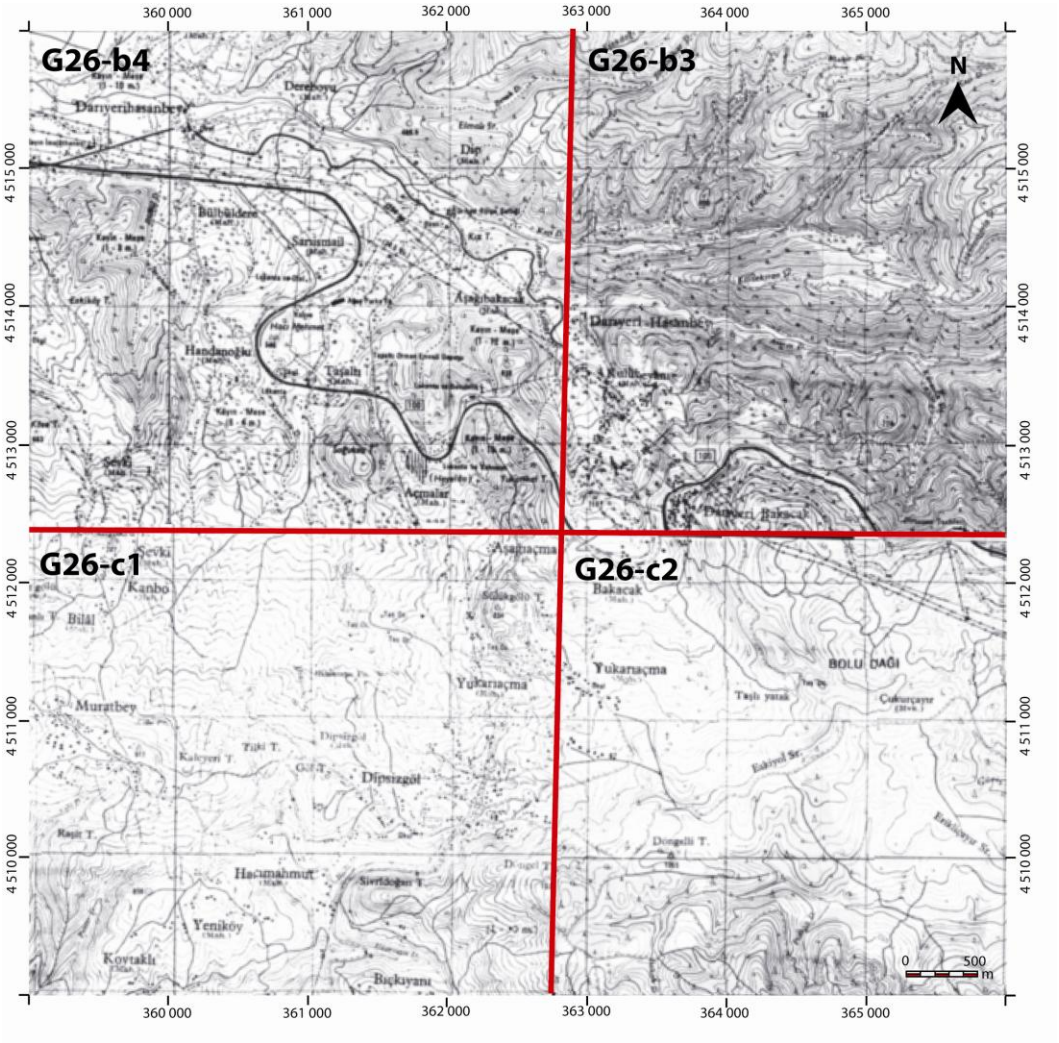

Figure 3.3. Topographic map of quadrangles G26-b3, G26-b4, G26-c1 and G26-c2 (1972 period).

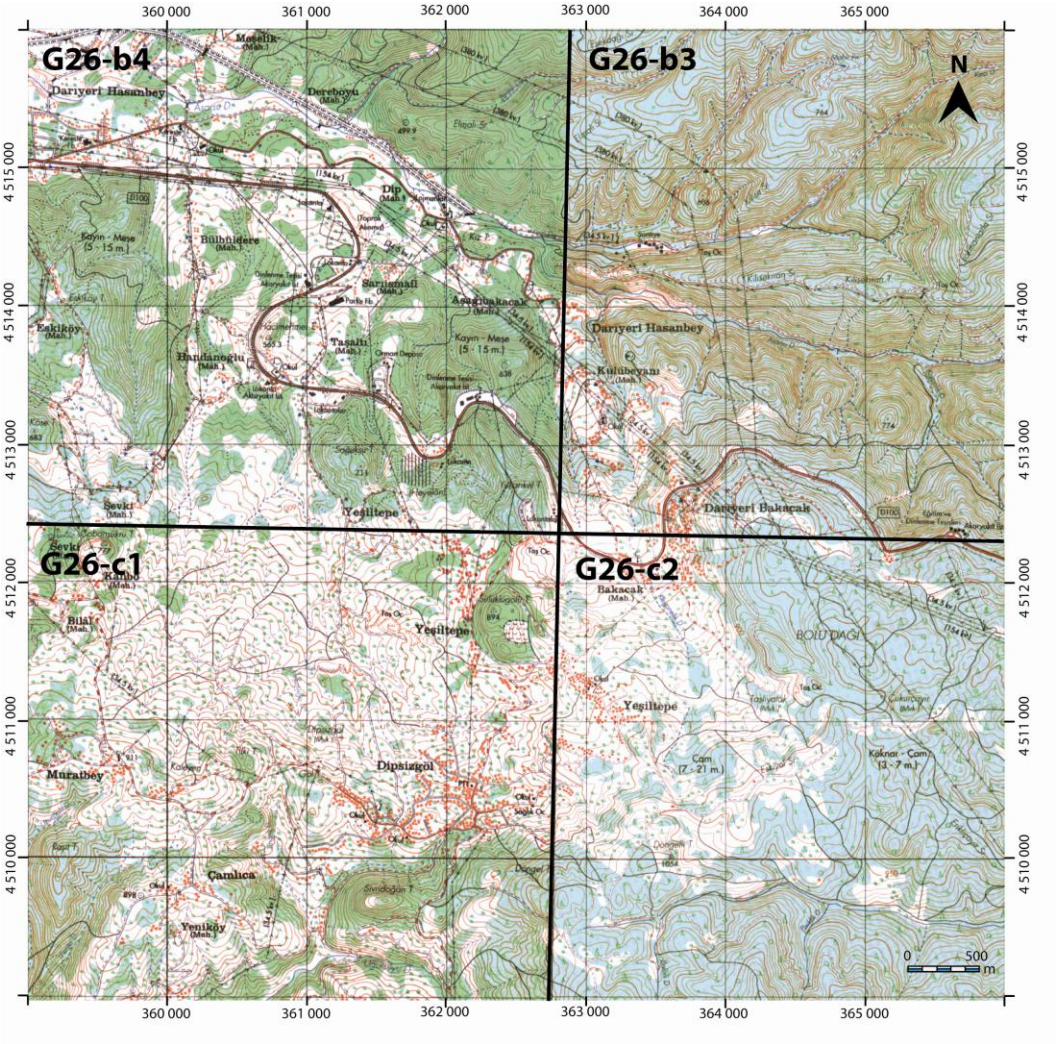

Figure 3.4. Topographic map of quadrangles G26-b3, G26-b4, G26-c1 and G26-c2 (1994 period).

3.1.2.3 Describing Camera Calibration Parameters

The transformation between object space and image space was eventuated in a camera with an image plane and a lens. Due to the distortion between object and image this transformation cannot be done perfectly. Therefore, in order to determine the orientation of the photographs camera calibration is a crucial requirement (Clarke and Fryer, 1998). For this reason, camera calibration parameters should be installed utilizing Match-AT software (Version 4.0.6). To do that, sine qua non (without which not) parameters that are camera type, focal

length of the camera, flight height, principal point of autocollimation (PPA) and distance between fiducial marks were inserted. However, for the years 1972 and 1984 due to some missing information in calibration reports, even nonexistent 1952 report, aerial triangulation process cannot be performed. For instance, the only camera information was the focal length and flight height for 1972 and 1984 sets, the lack of information about the fiducial marks and distortion information within camera plane hampered the calculations. Therefore, by using the parameters presented on Table 3.5 and Table 3.6, next step could be applied to only 1994 set.

Table 3.5. Camera calibration parameters of 1994 set of photographs.

Type of Camera	RC 10	
Focal Length	153.29 mm	
Flight Height	6050 m	
Principal Point of Autocollimation	**x (mm)**	**y (mm)**
	0.000	-0.006

Table 3.6. Calibrated data of fiducial marks referred to central cross for RC 10 camera.

	x (mm)	**y (mm)**
1	106.005	-106.002
2	-106.007	-106.004
3	-106.007	106.004
4	106.009	106.005

3.1.2.4 Selecting Aerial Photographs

To determine which photographs are covering the study area, the coordinates of principal points of all photographs were found. Then, on 1/25.000 topographic base, these points were plotted. In addition, by considering both the scale and the size, the photographs within the area under investigation were selected (Figure 3.5).

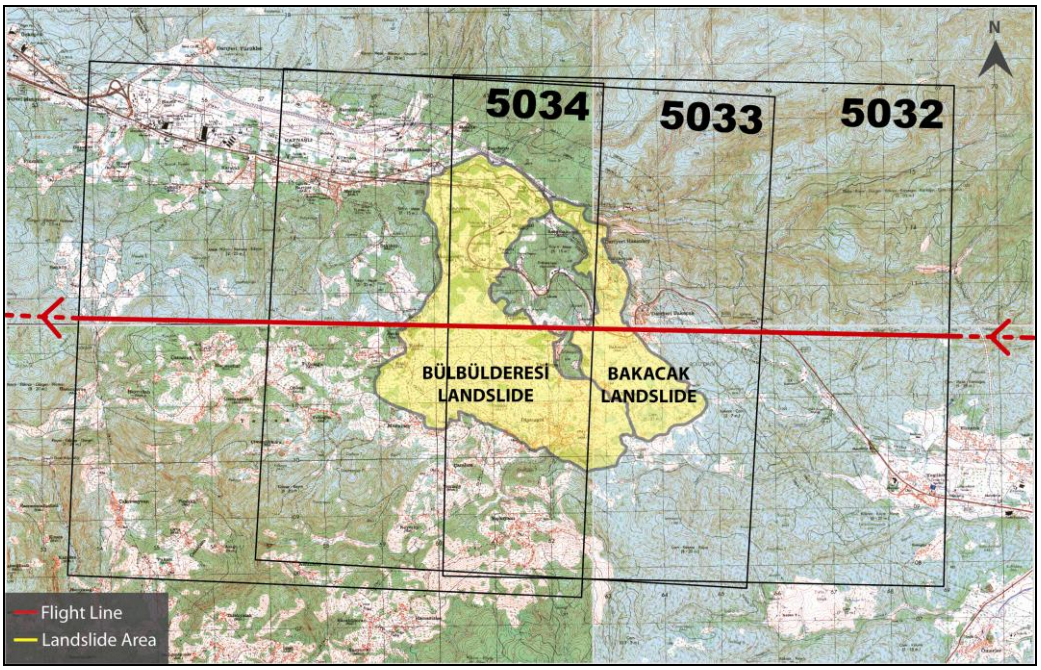

Figure 3.5. Aerial photographs that cover the study area.

3.1.3 Data Production

3.1.3.1 Block Adjustment

Before starting the aerial triangulation procedure, the strips include each row of photographs were created. Then, photographs in each strip were oriented and adjusted according to the flight direction (Figure 3.6).

3.1.3.2 Aerial Triangulation

Image orientation is a prerequisite for any project including photogrammetry. To determine the position and orientation of each photograph at the moment of exposure, it is necessary to perform aerial triangulation process that enables to convert image measurements into ground coordinates. The process was achieved by Match-AT software. Aerial triangulation composed of two steps that are interior orientation and relative orientation.

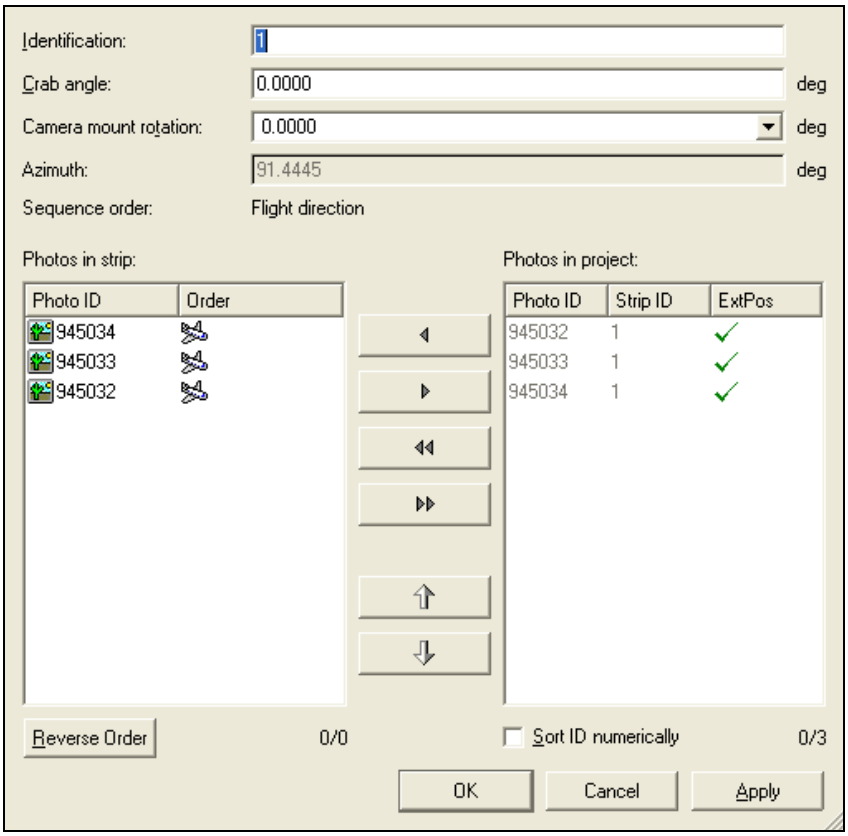

Figure 3.6. Created strip includes oriented photos.

3.1.3.2.1 Interior Orientation

The first step of aerial triangulation is setting up interior orientation. The purpose of interior orientation is to establish a relationship between pixel coordinate system and the image coordinate system (Karabörk et al., 2004). To achieve that, fiducial marks which are located either on the edge or in the corners of each air photos were marked manually. According to camera calibration report, location and numbers of fiducial marks were defined (Figure 3.7). As a result of interior orientation, RMS error was computed as 0.0107mm and shown in Figure 3.8.

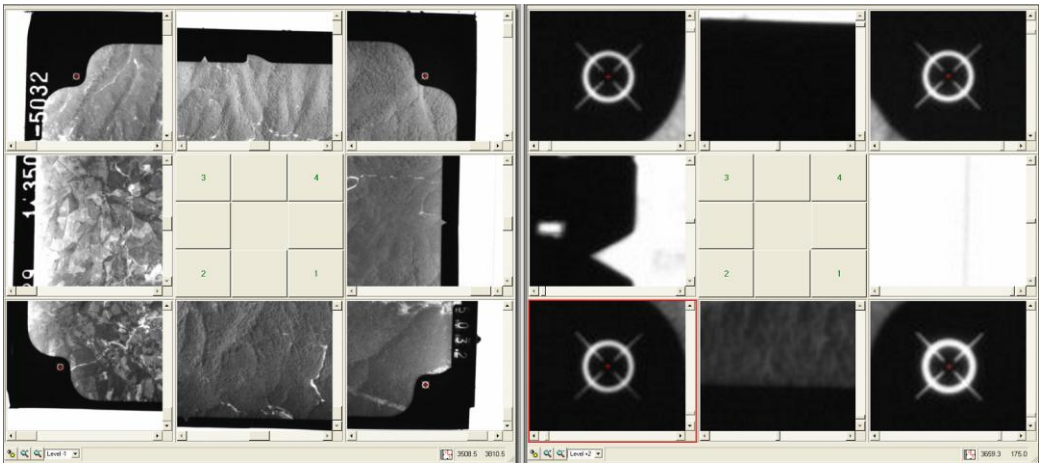

Figure 3.7. Orientation of the fiducial marks.

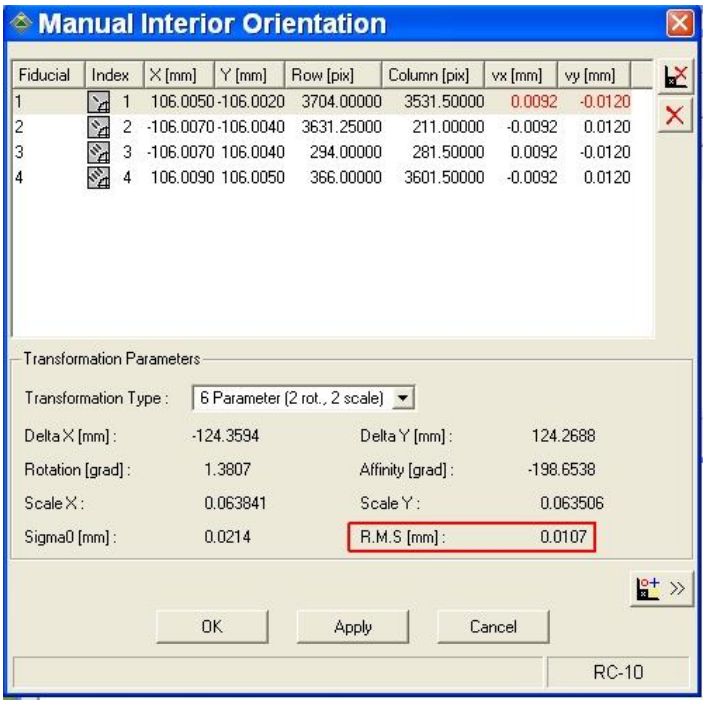

Figure 3.8. The RMS error value of interior orientation.

3.1.3.2.2 Relative Orientation

As the second step of aerial triangulation, relative orientation process is composed of collection of both ground control points (GCPs) and tie points.

Firstly, the coordinates of ground control points were determined by using 1/25.000 topographical maps. These points were collected from outside of the landslide area. The aim was to select check points in stable areas to enable to control the accuracy of relative orientation. However, collecting GCPs was quite difficult process in densely forested areas especially northeastern side of the study area. Because of this difficulty, the error in readings becomes larger. After selection, map coordinates of GCPs were imported as a text file. Then, the distributions of the points were auto generated on the images. To reduce the error, auto generated GCPs were adjusted manually according to corresponding map locations (Figure 3.9). Finally, individual RMS errors for each GCP and total RMS error were computed and shown in Table 3.7.

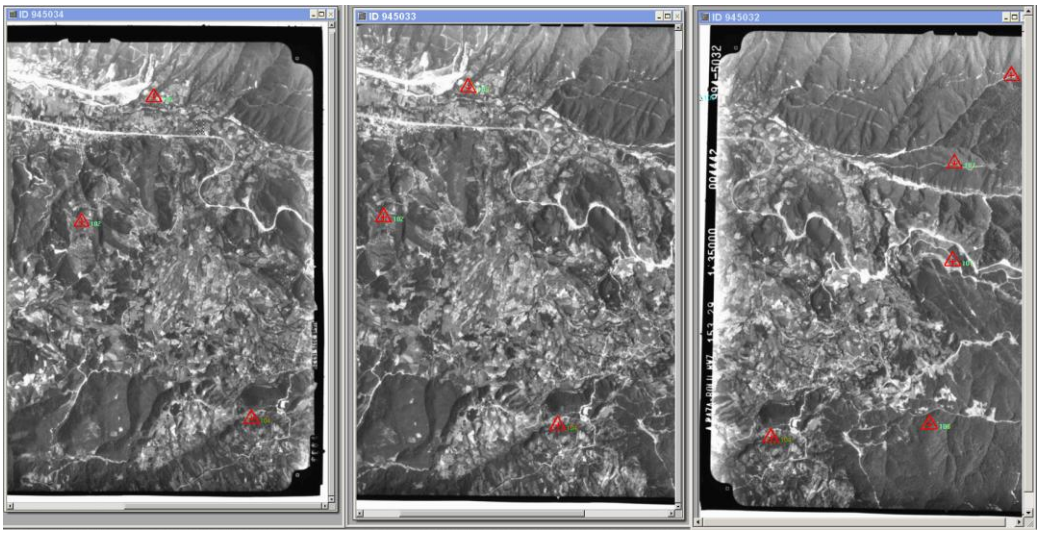

Figure 3.9. Collected GCPs (red triangles) are located on the photos.

Table 3.7. The RMS error values of the GCPs in x, y, z.

GCP ID	rx	ry	rz
101	0.874	0.981	-0.492
102	3.245	3.303	-0.774
103	1.932	-5.703	-1.677
104	-1.272	-1.391	1.285
105	-1.408	-2.003	-0.528
106	0.487	0.075	-0.936

After GCP generation, tie points were collected. The purpose of collecting tie points is to establish a rectangular extent and common orientation of the overlap area between the photographs. To obtain a stereo pair, the homogeneity and precision of the points' distributions have been considered while selecting these points. To achieve that, 19 tie points marked manually on common features like road junctions, stream intersections, field corners, etc. in both photographs at the corners, edges, and on the center lines of the overlap area. However like collecting GCPs process, at some areas collecting tie points has been limited in intensive forest area. Therefore, the results were negatively affected and the error in readings becomes larger. Then, automatic tie point generation process was applied (Figure 3.10). As a result of this process, 259 tie points were automatically collected. Until achieving high correlation values, editing locations of tie points were repeated.

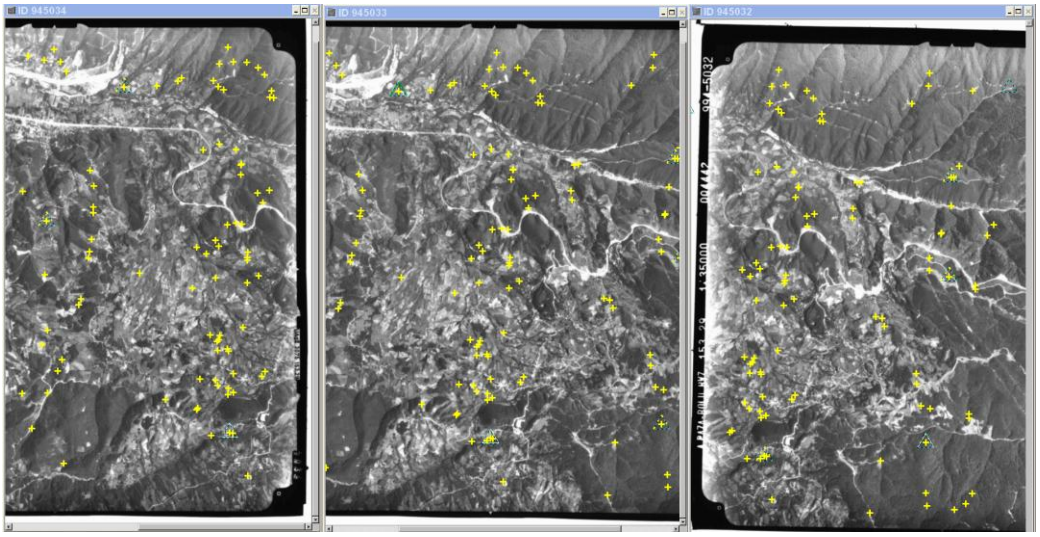

Figure 3.10. Automatic tie point (yellow dots) generation.

3.1.4 Data Extraction

3.1.4.1 Digital Photogrammetric Stereoplotting

Once the images have been oriented in a terrain coordinate system, stereoscopic vision and software stereo plotting tools can be used for contour generation. To do this, PHOTOMOD software (Version 4.1) was utilized. This process was entrusted by the expert operators. From the digital stereo images, contours were digitized in a 3D coordinate system and stored in a DGN file structure. In addition to contour data, elevation of some points were marked where contours cannot be plotted, for instance at steep slopes. Therefore, a vector data was generated so as to being a base for DEM extraction.

3.1.4.2 DEM Creation

A Digital Elevation Model can be defined as “a quantitative model of a part of the earth’s surface in digital form” (Burrough and McDonnel, 1998). DEMs are valuable basis for terrain representation and subsequent extraction of terrain related attributes (Weibel and Heller, 1991). Once necessary triangulation calculations have been completed and contours have been digitized, it was possible to obtain DEM of the study area. Digital Elevation

Model was generated with 10m interval by using Microstation V8 software (Figure 3.11, Figure 3.12). Furthermore, in this step TIN representation of the elevation surface was obtained in order to see how the current surface looks like (Figure 3.13).

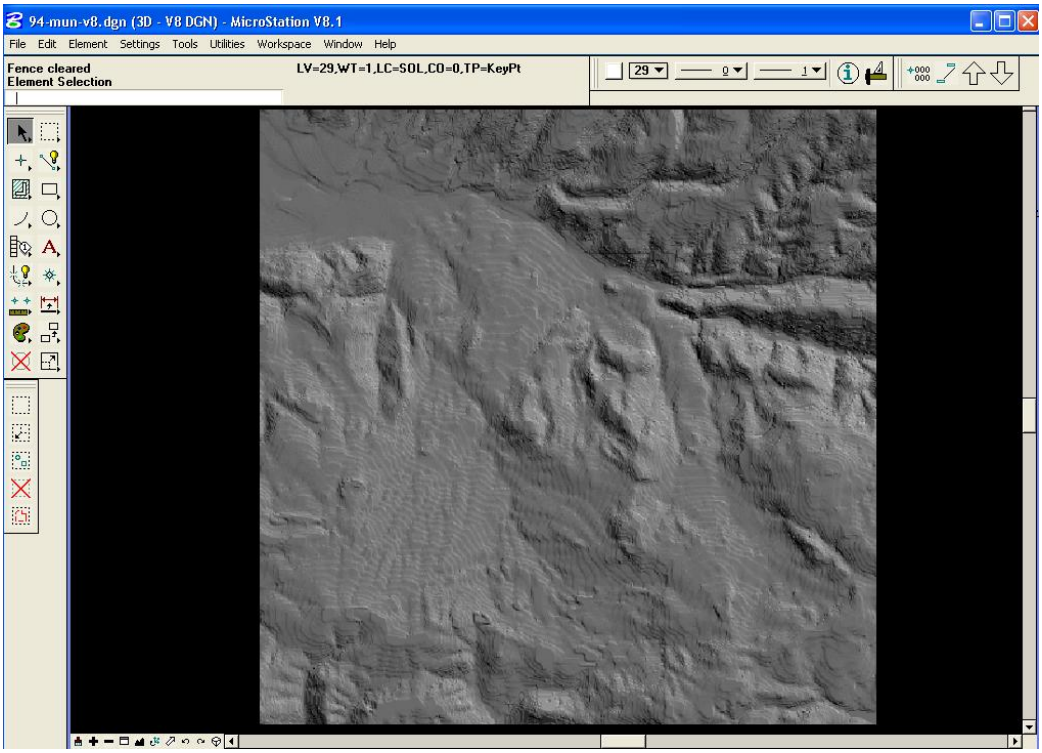

Figure 3.11. Top view of relief shading representation of DEM with an illumination angle of 45°.

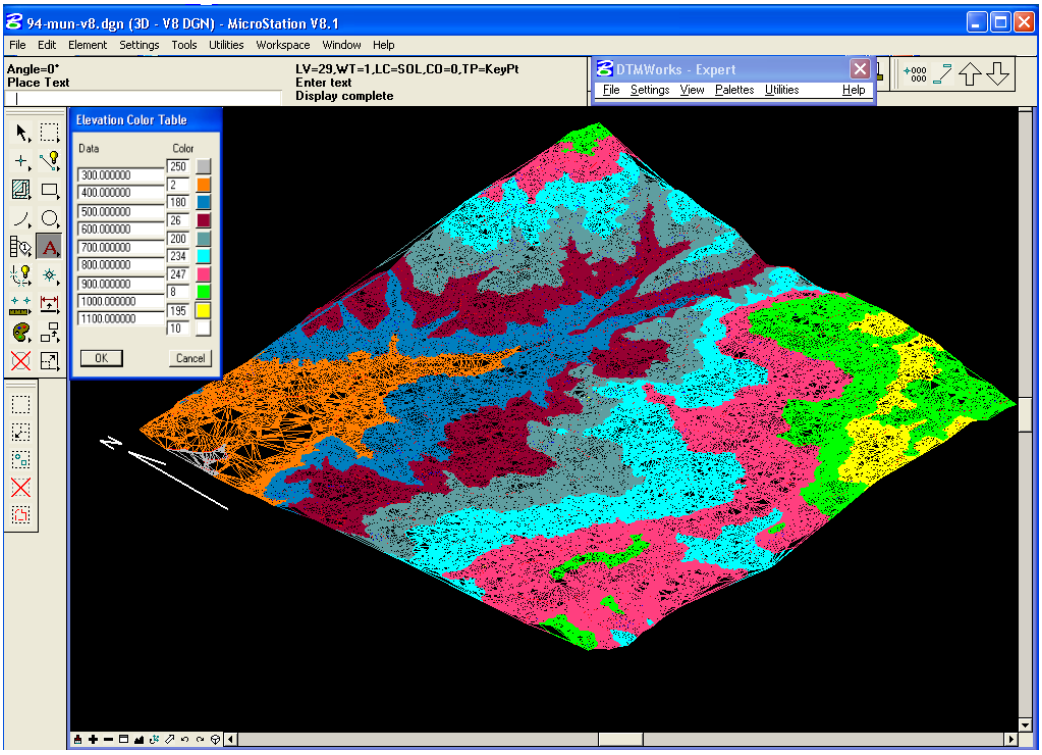

Figure 3.12. 3D perspective view of color coded DEM of the study area.

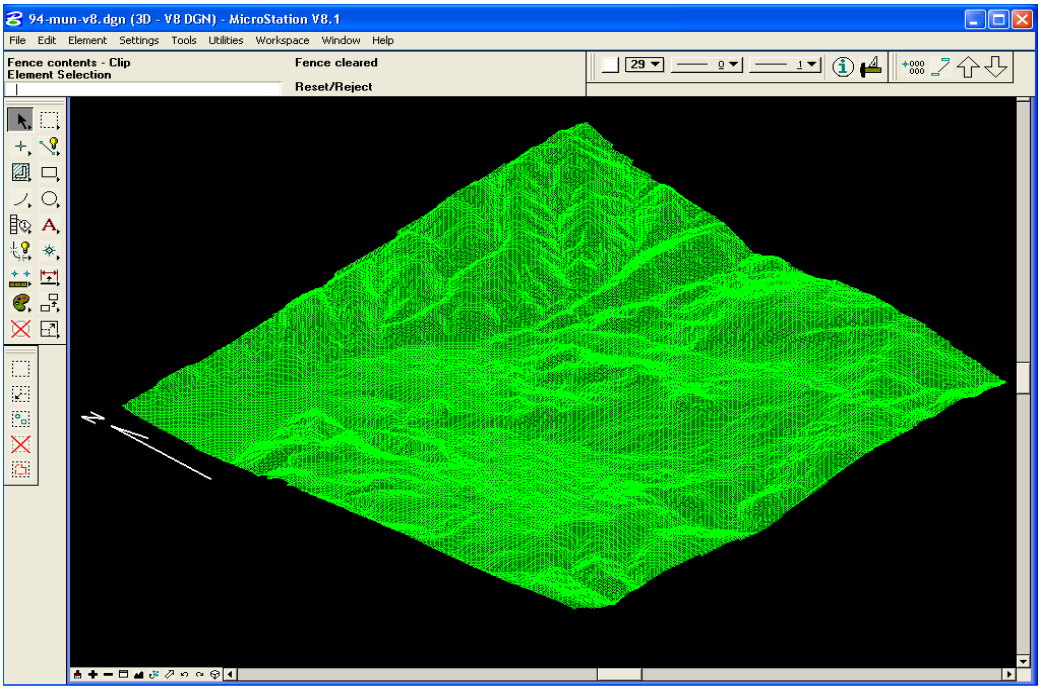

Figure 3.13. 3D perspective view of TIN.

3.1.4.3 Orthophoto Map Generation

Orthophotos were created through differential rectification, which eliminates image displacements due to photographic tilt and terrain relief so that all ground features were displayed in their true ground position. This allows direct measurement of distances, areas, angles, and positions (Wolf and Dewitt, 2000). In other words, orthophoto is an image where the perspective aspect of the image has been removed. Due to being planimetrically correct orthophotos can be used as maps (Mikhail et al., 2001).

To create an orthophoto, digital aerial photo pixels were projected to the specified orthophoto matrix through the assignment of a gray-scale value to each grid element of the DEM (Simard, 1997) (Figure 3.14). In other words, in order to generate an orthophoto map, previously generated DEM with its x, y and z data was imported as ASCII format on stereo image in PHOTOMOD software.

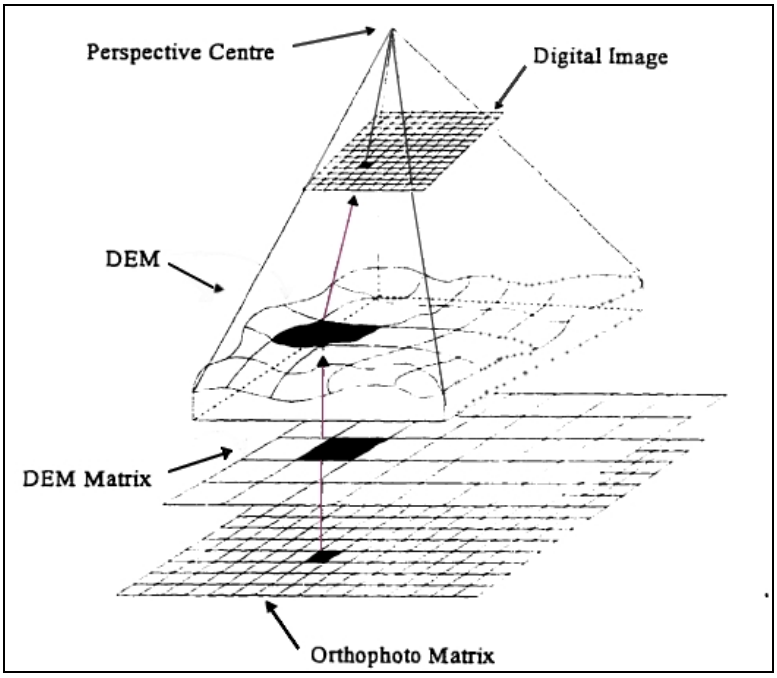

Figure 3.14. An illustration of the role of DEM in orthophoto generation (Simard, 1997).

Therefore, for 1994 year 1/10.000 scale digital orthophoto map with grids was obtained. This orthophoto will be used as a base map for aerial photo interpretation stage. Orthophoto map of the study area are shown in Figure 3.15 and Figure 3.16.

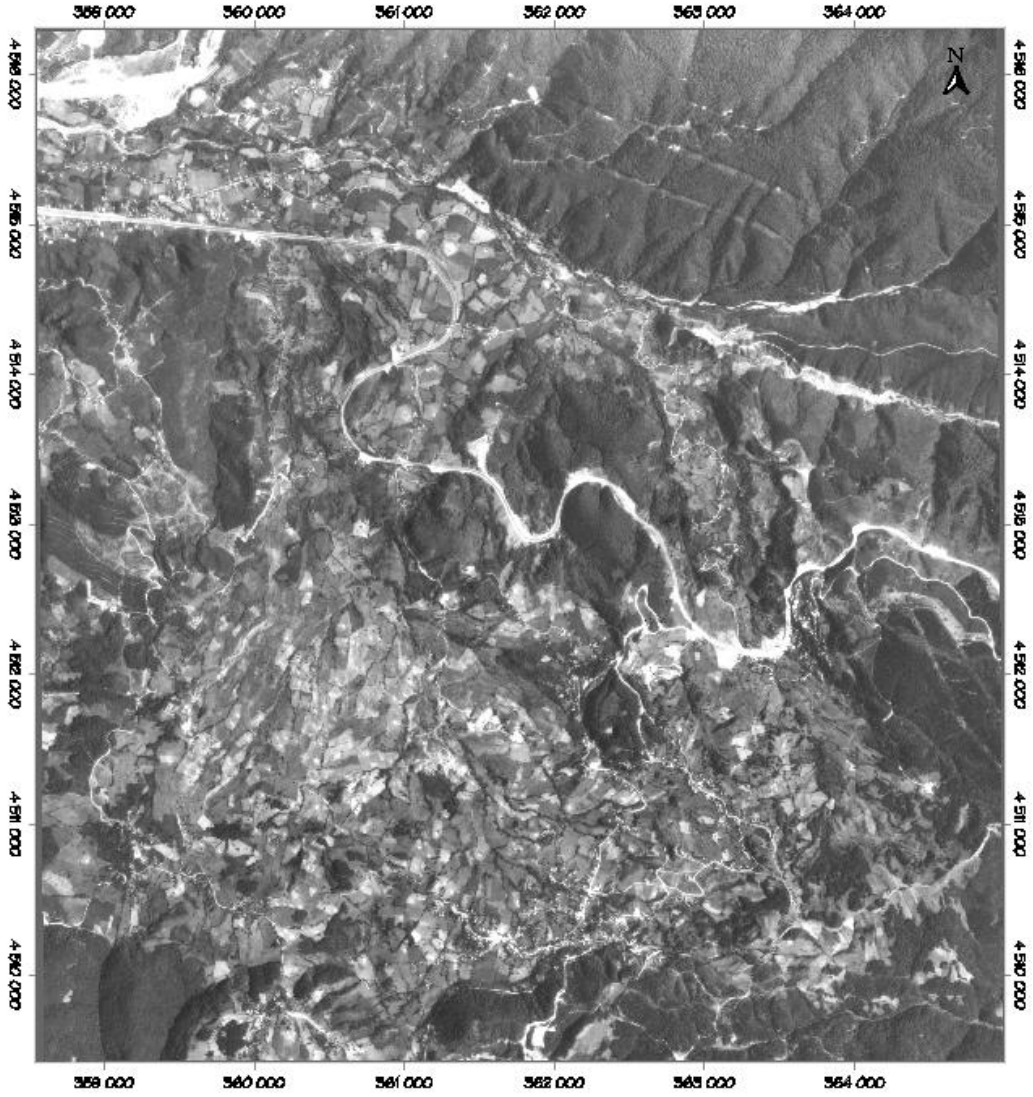

Figure 3.15. 1/10.000 scale orthophoto map of the study area.

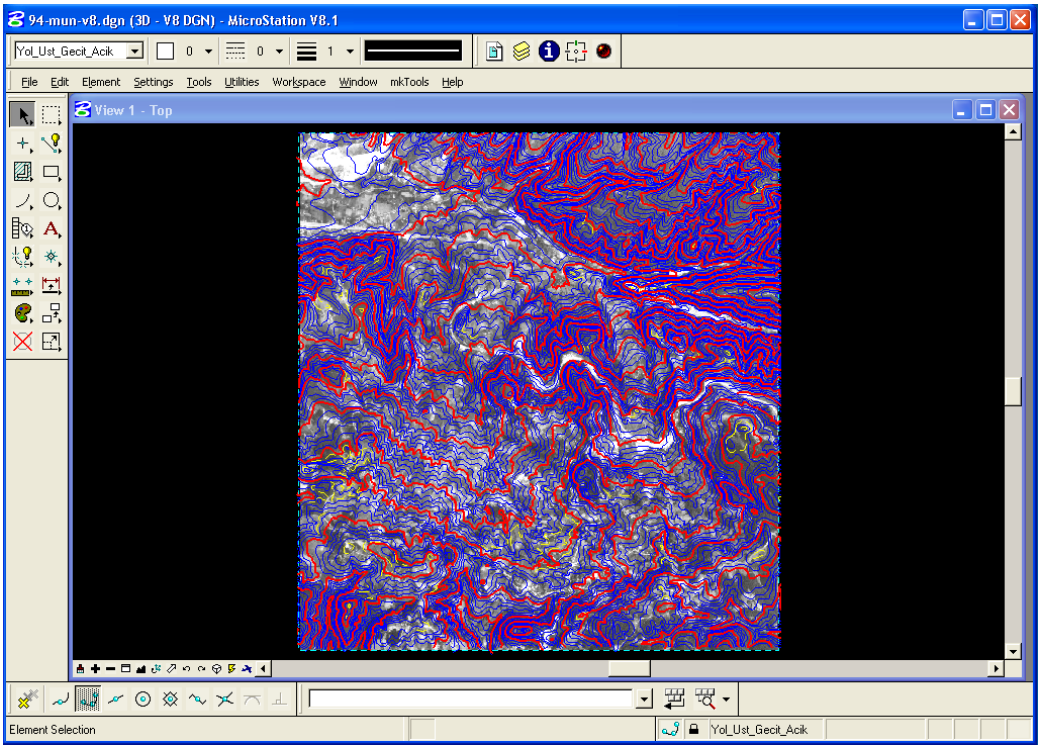

Figure 3.16. 1/10.000 scale orthophoto map with contours.

3.2 DEM DIFFERENCE

3.2.1 Data Production

After generating DEM of 1994 period, our next stage was to create DEMs for both 1952 and 1972 period in order to reveal the surface change between these years. Both due to lack of 1984 topographical maps and absence of camera calibration reports of this periods' aerial photographs, no DEM could be made available for this stage.

3.2.1.1 Contour Data Generation

Due to the lack of camera calibration parameters except 1994 period, DEMs corresponding to 1952 and 1972 could be only generated by digitizing topographical maps of these years. To achieve this, previously scanned 1/25.000 scale topographical maps corresponding to 1952 and 1972 years were digitized

by utilizing ArcMap software (Version 9.2). Therefore, contour data of two epochs were obtained.

3.2.1.2 DEM Creation

After, obtaining the contour data corresponding to 1952 and 1972 period, by utilizing TNTMips software DEMs of these years were acquired.

3.2.2 Data Extraction

3.2.2.1 DEM Difference

In this stage our aim was, to find the differences between the DEMs of 1952, 1972 and 1994. During this stage, in order to achieve standardization through the three DEM, these DEMs belong to three different epochs were resampled by utilizing TNTMips software. This resampling was vital to fix the extents and the centers of the pixels. After that, to extract the ground change between 1952, 1972 and 1994, each DEM was subtracted from previously dated one. In the differential image, the points of a minus value displayed as red showed decrease of the elevation values whereas, the point of a plus value displayed as blue showed increase of the elevation values. In other words, as we expected toe of the landslides should be displayed with red where the elevation had been increased. On the contrary, at the head/scarp zone of the landslide the elevation should be decreased and displayed with blue. The points of value 0 displayed as white showing no significant ground differences occurred between corresponding years (Figure 3.17A, B and C). However, when the DEMs were compared with each other, it was realized that especially at the intersection parts of 4 sheets there were some abnormalities. It was because of the inconsistency between sheets of 1952 and 1972 periods due to the difference in production dates (Table 3.2 and 3.3). Therefore, the change in the surfaces if there exists any could not be detected by the subtraction of DEMs.

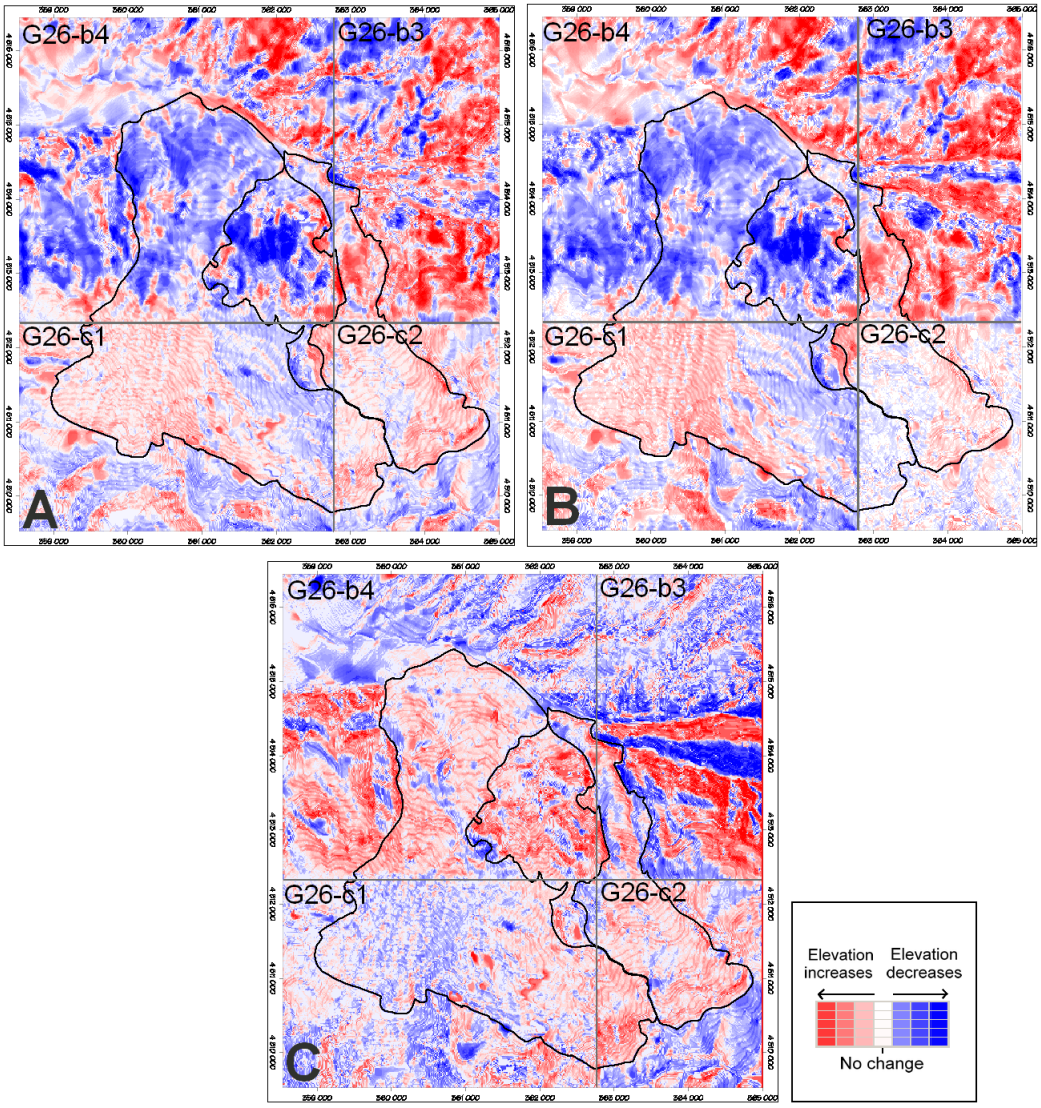

Figure 3.17. Differential DEMs. (A) Difference of 1952-1994 period; (B) Difference of 1952-1972 period; (C) Difference of 1972-1994 period.

3.2.2.1.1 Landslide Morphology

The only resulting DEM coverage corresponds to 1994 over the study area was adopted to identify the characteristics of Bülbülderesi and Bakacak landslides. The task has been implemented in TNTMips software (Version 6.9) which enables to display the profiles of these landslides. On the basis of analysis of shape and morphology, cross-sections obtained from different parts of the landslides were examined (Figure 3.18).

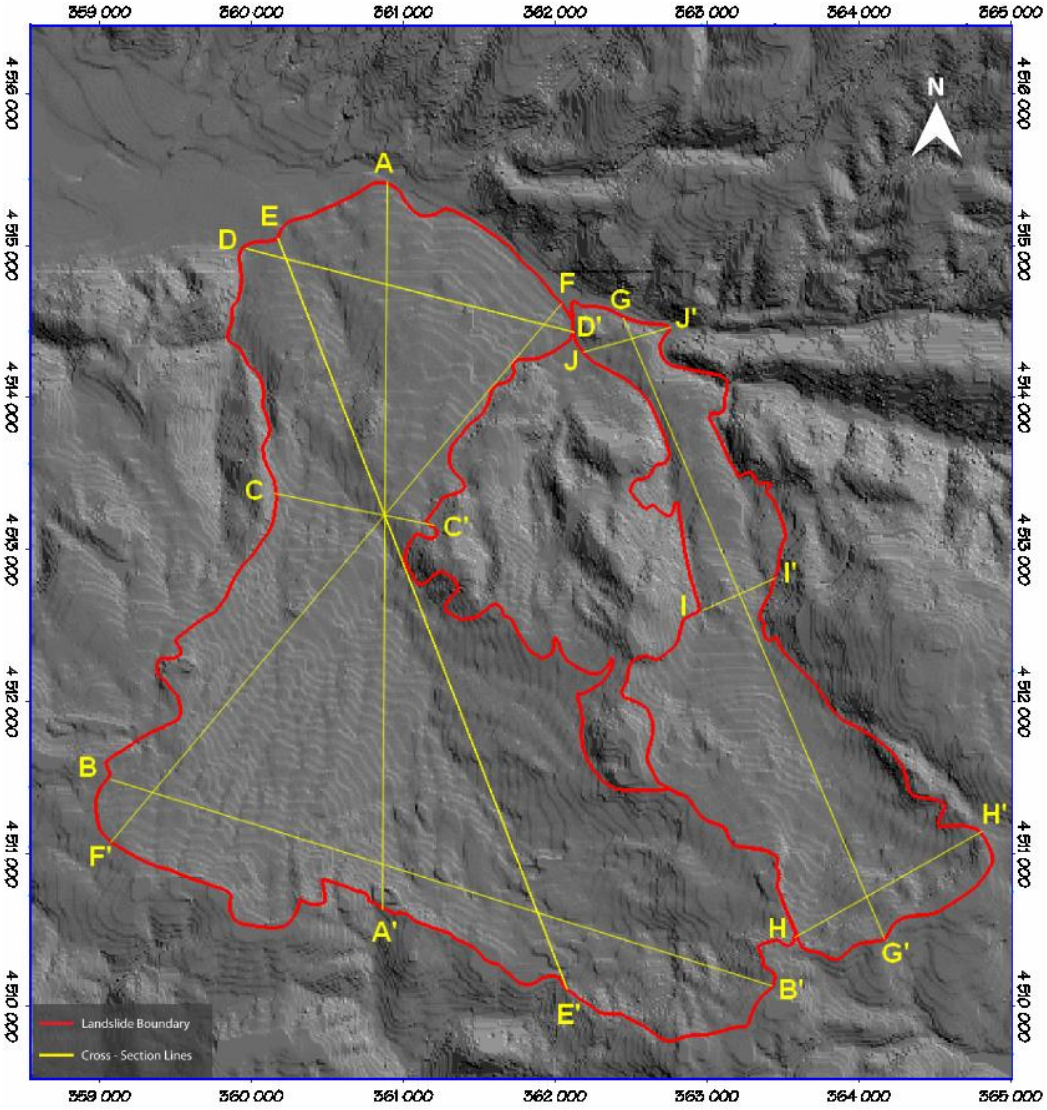

Figure 3.18. Cross-sections extracted from DEM on plan view.

Based on the profile from toe to crest of the Bülbülderesi landslide, the approximate length was measured as 4773m whereas the approximate width was about 2614m. Total elevation difference from crest (831m) to toe (349m) of the landslide was 482m along an axis parallel to the average movement direction (Figure 3.19A-A'). The extent was calculated as ~12km^2 having an approximate slope gradient between 10-15° with local variations. The highest point along the head of the landslide was at an elevation of about 1036m, whereas, the base of the head was at about 769m in elevation (Figure 3.19B-B'). At the neck where

width of the landslide reaches its minimum value, the elevation decreases east to west and ranges in between 518m to 601m (Figure 3.19C-C'). In the toe zone the east part is again more elevated than the west part and the altitude varies from 338m to 443m (Figure 3.19D-D'). In addition, when the Bülbülderesi landslide was examined diagonally, Figure 3.19E-E' and Figure 3.19F-F' were extracted. The elevation differences along profiles from crest to toe of former was 496 and in latter was 482. It is seen in the cross-sections that the east side of the landslide is always elevated more than that of its west side. The main direction of the movement was toward north-east.

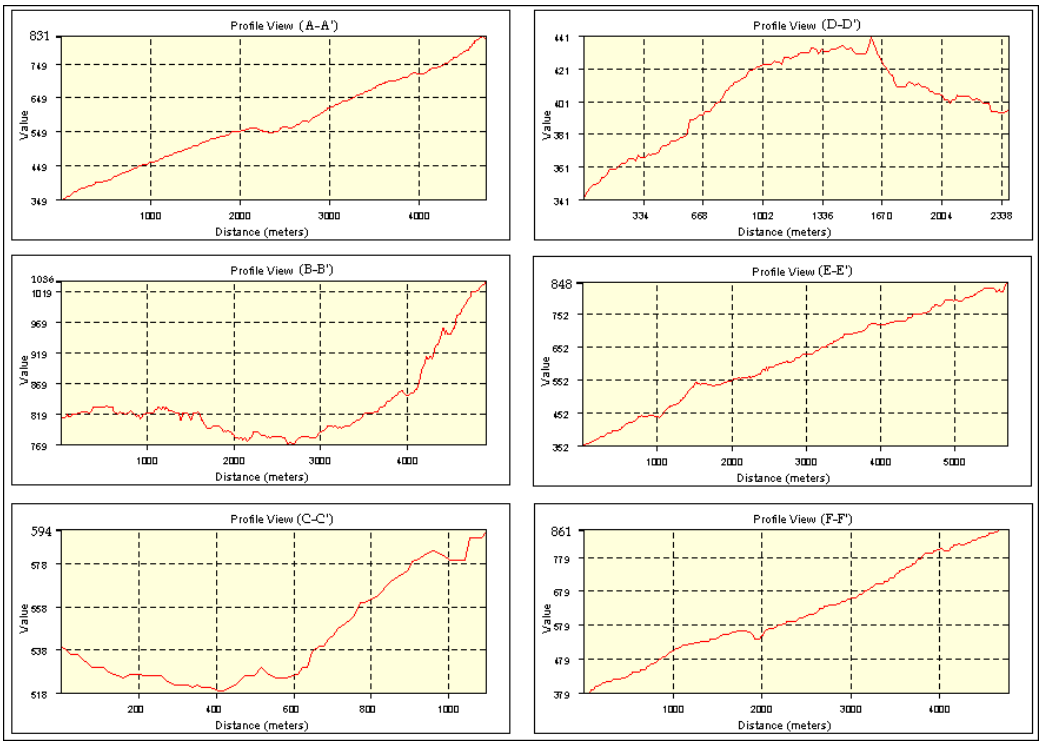

Figure 3.19. Profile views of Bülbülderesi landslide along A-A', B-B', C-C', D-D', E-E' and F-F' on plan view.

On the other hand, the approximate length of the Bakacak landslide was 4420m and the approximate width was 832m with an area of ~4km^2. Total elevation difference from crest to toe of the landslide was 622m where minimum altitude was 399m and maximum altitude was measured as 1021m (Figure 3.20G-G'). The measurement was taken to approximate the best

possible center line of the mass movement with an approximate slope angle 9-14°. Measured elevation values ranged between 948m to1003m along the profile on the head (Figure 3.20H-H'). The neck of the landslide was measured as 554m width where the total elevation difference was 54m (Figure 3.20I-I'). The maximum elevation at the toe where the landslide piled material was 435m (Figure 3.20J-J'). The main direction of sliding was toward north-west.

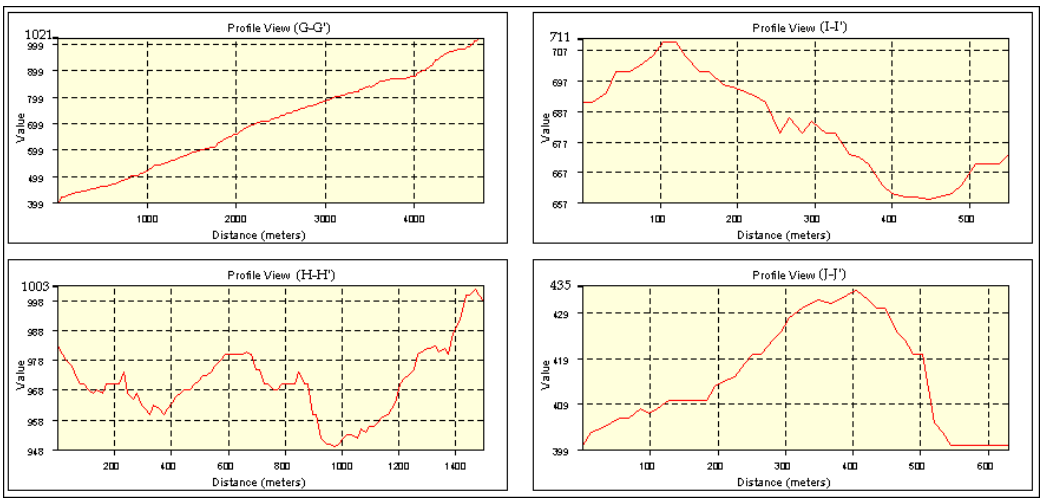

Figure 3.20. Profile views of Bakacak landslide along G-G', H-H', I-I' and J-J' on plan view.

Asarsuyu, Elmalık and Kızılsu are the main surface waters of the study area and its close vicinity. To understand the drainage characteristics of the study area another product of DEM that is watershed analysis was utilized. One of the products of watershed process was the flow path vector that shows the network of stream channels drain each minor watershed. The flow paths which constitute the drainage system forms a well displayed parallel drainage pattern within landslides (Figure 3.21). Another product was watershed boundaries that follow topographic divides between drainage systems. When it was examined it was also seen that the majority of the boundary of landslide coincides with drainage divides especially in crown regions.

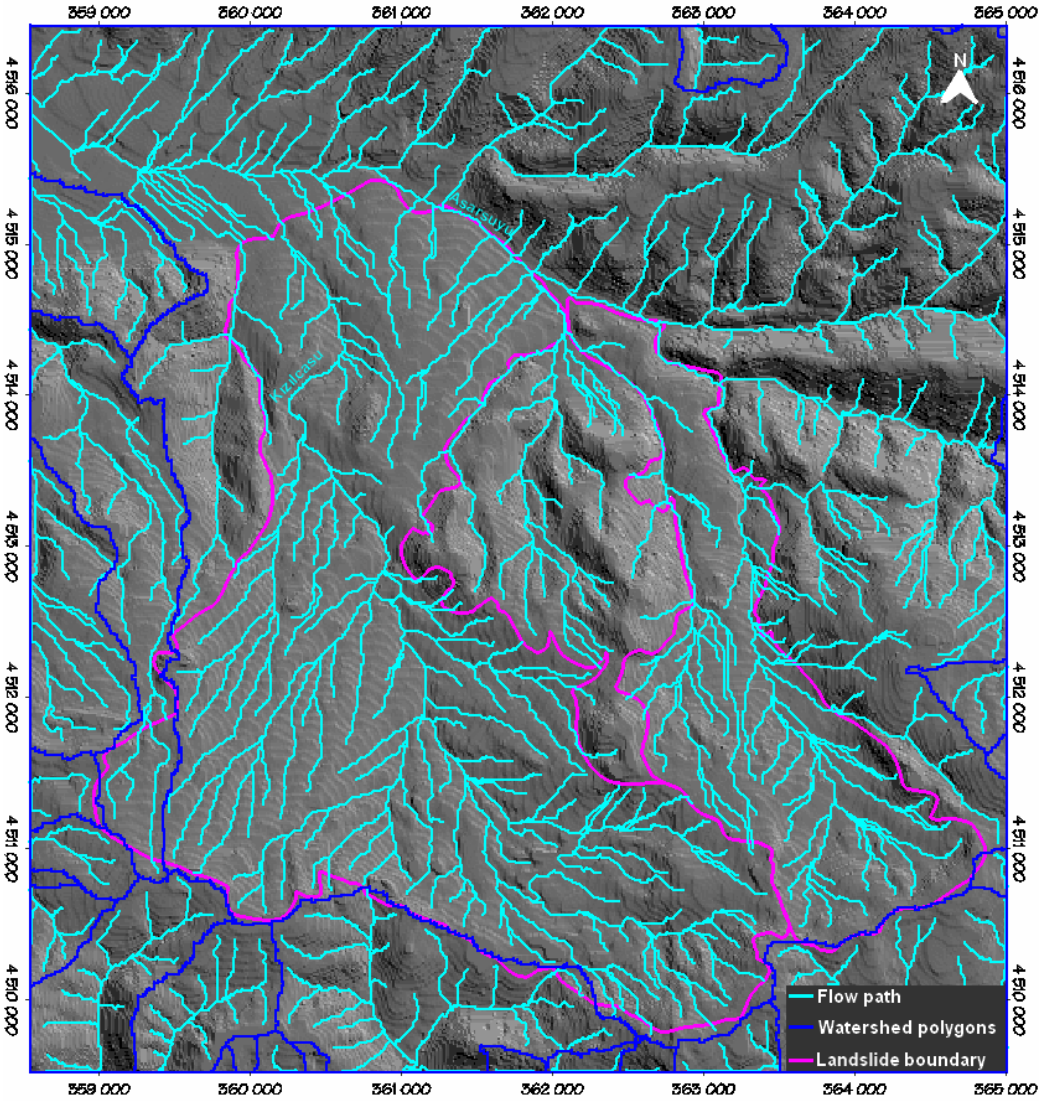

Figure 3.21. Flow paths and watershed polygons with landslide boundaries.

Based on the geological and geotechnical studies performed in literature (Işın, 1999 and Süzen, 2002) and with field studies some significant information about the sliding material was obtained. Not only the flyschoidal character of the lithologies but also the presence of significant amount of gypsum affects the landslide. Gypsum can be dissolved by surface or groundwater forming karstic depressions. These depressions vary from 1,5 to 2m in diameter and 10 to 15m in depth. There were many pit holes that were formed by dissolution of gypsum and many surface flows disappear here joining to groundwater. As a result of

this continuous recharge, stability was affected in a negative way. Apart from these depressions, gypsum quarries could be detected in aerial photos (Figure 3.22).

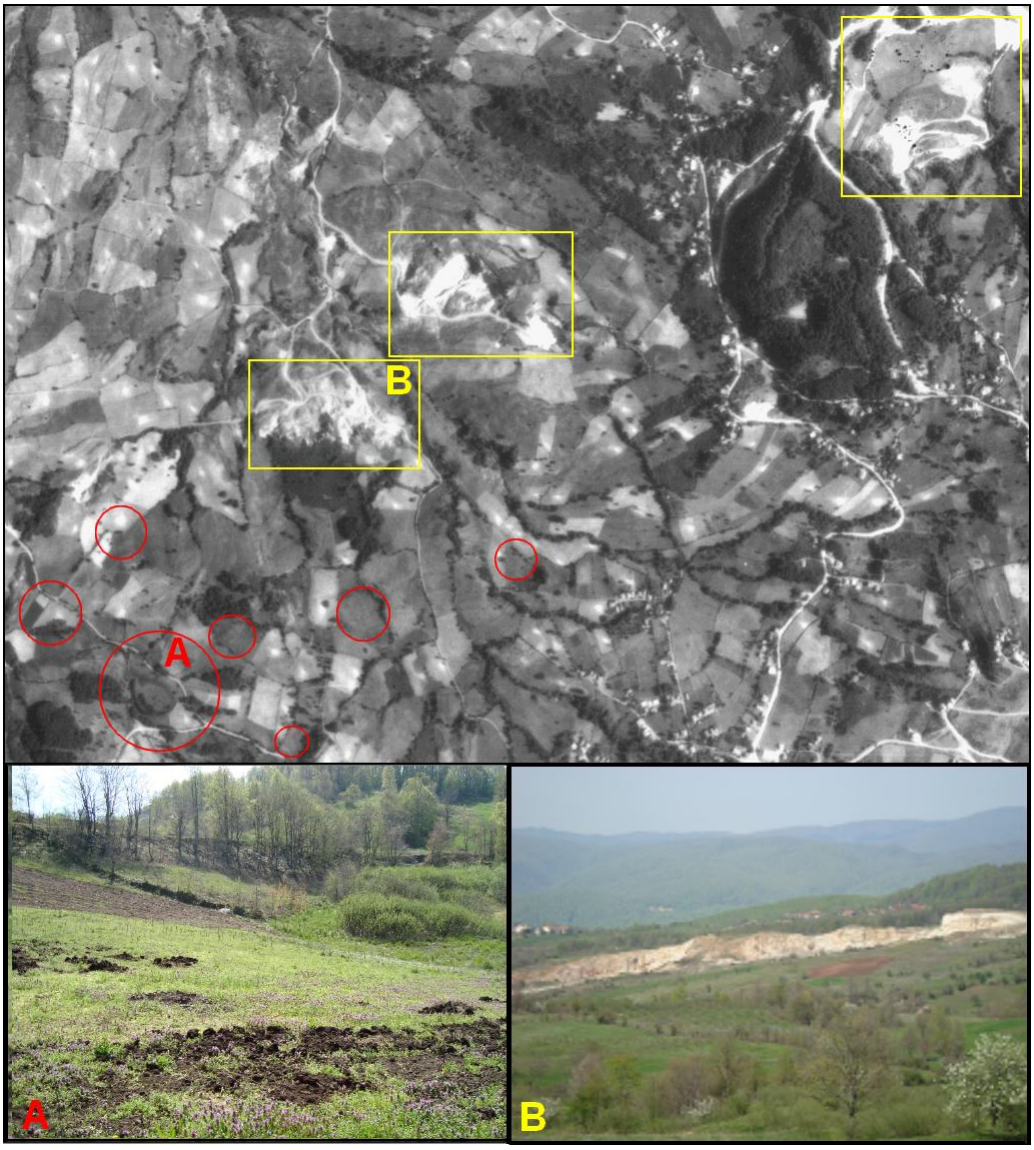

Figure 3.22. Karstic depressions represented by red circles (A) and gypsum quarries displayed as yellow rectangles (B).

3.3 VISUAL INTERPRETATION OF AERIAL PHOTOGRAPHS

3.3.1 Data Acquisition

Because of the fact that it was unable to achieve monitoring the surface changes either by orthophoto production or by utilizing DEMs, a new method had to be developed that was the visual interpretation of aerial photographs. At this stage, previously produced orthophoto map was used as a base map in order to transfer the interpreted information on this map.

3.3.2 Data Production

3.3.2.1 Aerial Photograph Interpretation

Aerial photo interpretation is one of the most useful and effective method used in the recognition and classification of landslides. This process provides not only 3D view of the terrain but also 'birds eye' perspective obtaining local to regional view of landscape. In this study, multi-year aerial photographs were used for assessing long-term evolution of the Bülbülderesi and Bakacak landslides. The availability of multiyear aerial photo coverage helped to assess the morphological changes that occurred between 1952 and 1994. In other words, aerial photo interpretation was used to investigate the activity of the Bülbülderesi and Bakacak landslides in 42 years. The purpose of the process is to gather the information for monitoring the movement of the landslides, to define the size and the extent of the main boundaries and to determine the movements within the landslide bodies since 1950's. This methodology consists of an analogue photo interpretation by means of a mirror stereoscope. To do this, 1/10.000 scale orthophoto map that has been produced previously was used as a base map, of which all interpretations are transferred. While the interpretation on several aerial photographs ranging from year 1952 to 1994 was executed, first of all boundaries of the 2 main slides were determined and transferred to the base map on a transparent overlay. After this, a detailed study was carried out within the boundary of the landslides. In this context,

topographical changes that can be recognized on photos were delineated and interpreted information was transferred to the base map to assure geometric accuracy and to provide the possibility for quantitative comparison of the maps obtained from different epochs. In other words, surface alternations such as slope instabilities, vegetation removal, manmade structures, etc., were detected. In the end of visual interpretation all of the maps were scanned. After scanning, these drawings were digitized by utilizing ArcMap software. The results have shown that there is not a major movement on the boundaries of Bülbülderesi and Bakacak landslides, except some minor differences. However, within these landslides there were many topographical changes that can be obviously seen. These changes would be explained in detail regarding to 1952, 1972, 1984 and 1994 periods separately in the following sections. Detectable surface changes outside the boundaries were transferred onto the base map however; they were not taken into consideration and represented as yellow on the activity maps.

3.3.2.1.1 Interpretation of the Aerial Photographs from 1952 Period

Unlike usual E-W flight direction, in 1952 the flight line was NW to SE (Figure 3.23). The flight altitude was 4200m. The aerial photographs that cover the study area consist of 3 strips of the flight number 381 according to the flight plan. The first strip includes 4 photographs that are 688, 687, 686 and 685. The second strip consists of 652, 653, 654, 655, 656, 657 and 658. The last strip corresponding to flight number 381 comprise photographs 623, 622, 621, 620, 619 and 618. Total number of interpreted photographs is 17. These aerial photographs have some common characteristics such as, 1/20.000 scale, black and white print and 17,5 x 17,5 cm size.

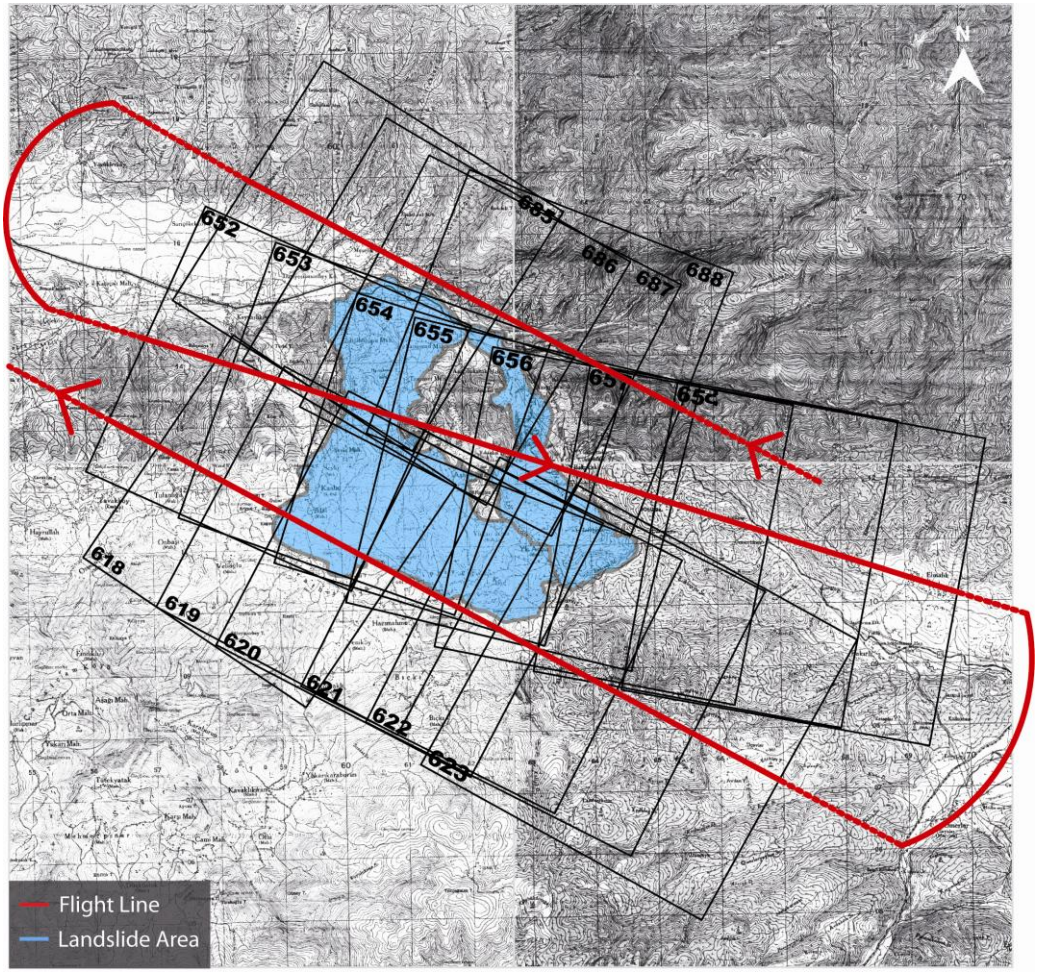

Figure 3.23. Flight plan of 1952 period on 1/25.000 scale topographic maps.

Since there were no aerial photographs prior to 1952, analysis of the Bülbülderesi and Bakacak landslides will start with this period. To examine the morphological changes, first of all the main boundary of these landslides were drawn. Drawing the body of the landslides was not complicated. However, at some parts of the scarps where the failure was effectively generated, it was very difficult to determine where the boundary should be passed in 3D view. Not only the karstic depressions due to presence of gypsum but also the presence of intense forest areas especially at south-east part of the Bülbülderesi landslide makes it quite hard to draw the boundary.

When the Bülbülderesi landslide examined in detail, it was obviously seen that, there were lots of flows at downslope of the main scarp (Figure 3.24A). The flow direction of most of the slides was NNE (north, north-east). At the western side of the crown of main slide, scarp traces of minor slides directed to north were detected (Figure 3.24B). However, slides at the eastern side of the crown directed to west and northwest (Figure 3.24C). Moreover, a number of rotational slide masses were extending downslope. At the right flank, revealing a typical flow pattern, some significant movements have been observed (Figure 3.24D). Particularly, a mottled texture due to presence of gypsum was remarkable (Figure 3.24E). At the foot and toe of the slide where the area is denominated as "zone of accumulation" according to Varnes (1978), some debris flows and slides could be seen (Figure 3.24F_1, F_2).

Besides, 1952 photos reveal that there were a number of surface movements on another large landslide Bakacak. At the crown of the Bakacak landslide, scarp traces of minor slides could be observed (Figure 3.24G). The major movement was detected on the main body. In the middle of the main body debris flows could be interpreted (Figure 3.24H). Particularly in the center of the main slide, a large volume of material coming from the slide masses above on which secondary scarps were developed (Figure 3.24I). Like in the Bülbülderesi landslide, mottled texture in some parts of the Bakacak landslide was noticed (Figure 3.24I). Furthermore, at the right flank sliding masses could be detected (Figure 3.24J). Not only on depletion zone but also on accumulation zone minor slides could be interpreted (Figure 3.24K).

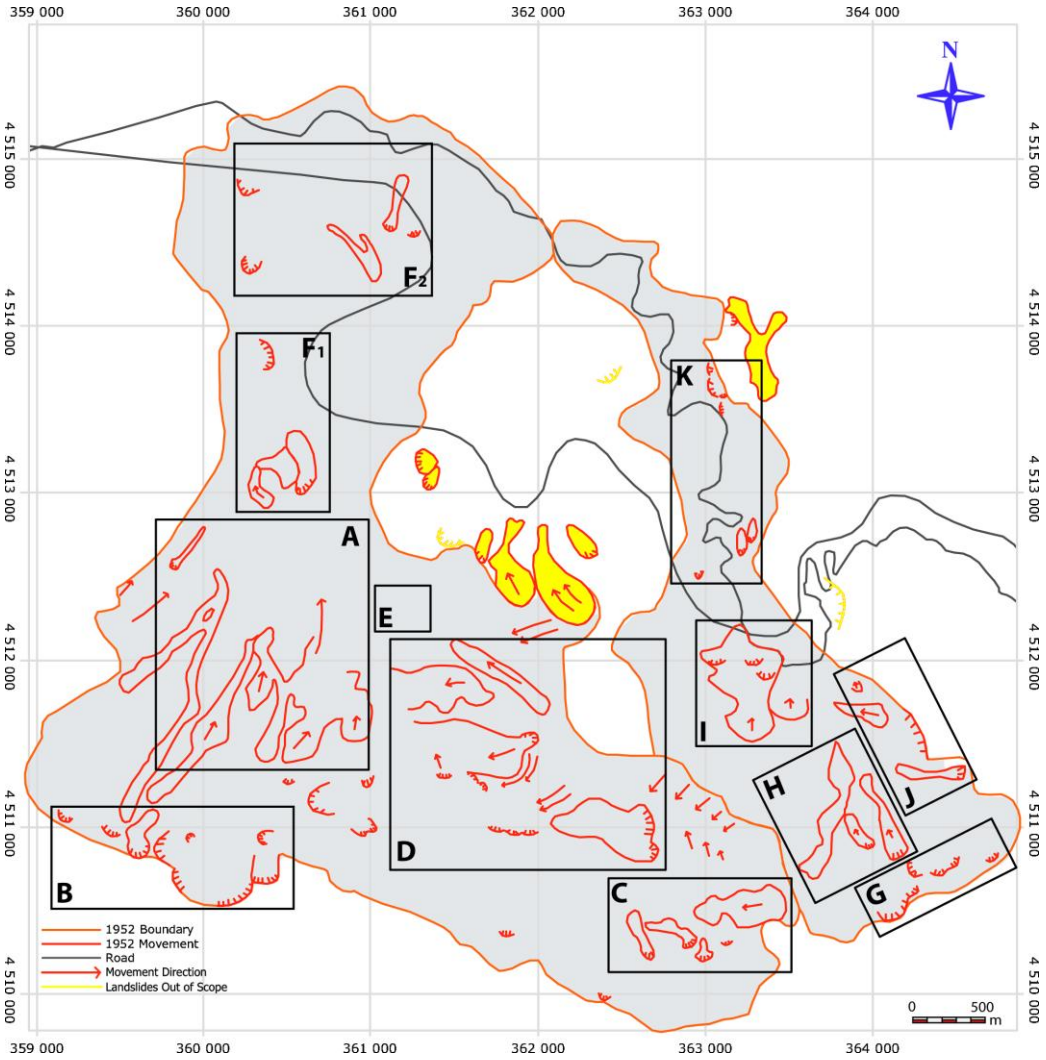

Figure 3.24. Digitized landslide activity map of 1952 period.

3.3.2.1.2 Interpretation of the Aerial Photographs from 1972 Period

According to the flight plan of 1972 year, at 4500m the flight was performed in usual E-W direction with the flight number 2641 (Figure 3.25). Area coverage is built up by flying 2 strips. The first strip consists of 5 photographs that are 1228, 1229, 1230, 1231 and 1232. The second strip corresponding to flight number 2641 includes the photos number 1249, 1248, 1247 and 1246. Total 9 photographs were interpreted. These are black and white print. Unlike 1952 photos, the scale of 1972 photos is 1/25.000 and the size is 23 x 23 cm.

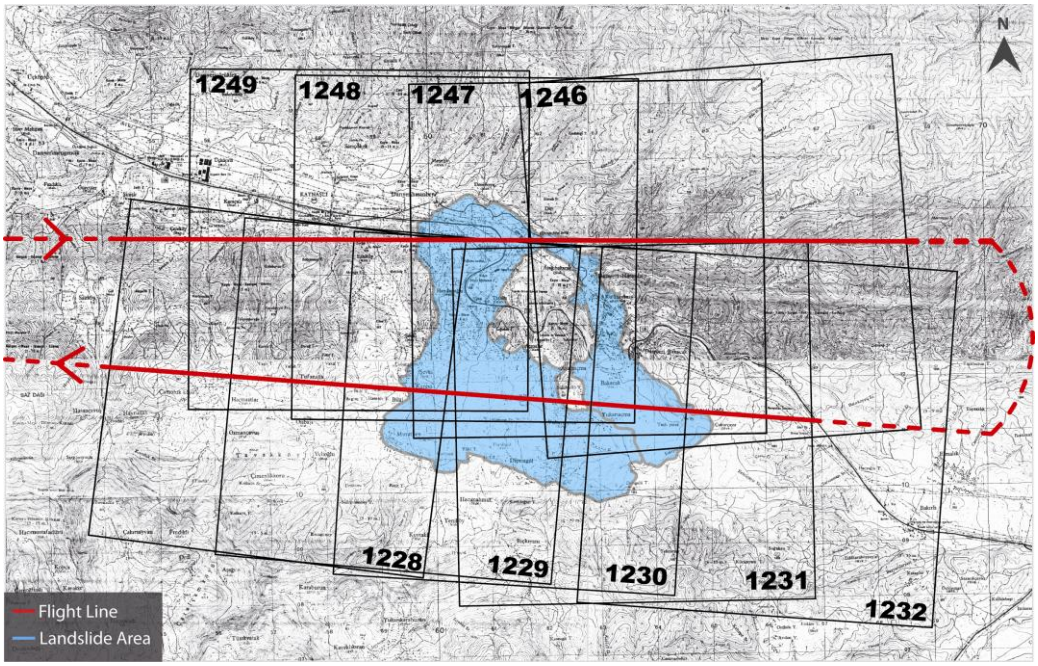

Figure 3.25. Flight plan of 1972 period on 1/25.000 scale topographic maps.

In 1972 photos it was visible that, flows on the main body of the Bülbülderesi landslide could be still detected. However, some parts of the flow extending downhill disappeared due to agricultural activities and erosion. Therefore, drawing the boundary of the flow was impossible. On the other hand, between the years 1952 and 1972, some new slides were developed on the main body. Also, some parts of the flow retrogressively advanced towards the main scarp of the Bülbülderesi landslide which indicates an activity on the main body (Figure 3.26A). Unlike new developing slides, the traces of some old slides at the main crown were totally vanished (Figure 3.26B and C). In addition, the downslope movements of right flank could be still observed. However, the boundary of the slide located at the southern part of Sülüklügölü Hill could not be noticed anymore. At this point, a debris flow detected on the right flank showed a progressive movement (Figure 3.26D). This is an evidence of still continuing activity. At the zone of accumulation, a major movement could not be observed. However, some slides were vanished at the center of the foot and eastern parts of the toe. Particularly, retrogressive movement of a debris flow at

the toe was recognized (Figure 3.26E_1, E_2). Moreover, new landslides were developed at the right side of the foot (Figure 3.26F).

On the other hand, at the surface of the Bakacak landslide no major morphological differences from 1952 could be observed, except some vanished flows at the eastern flank and developed slides at the zone of depletion (Figure 3.26G). Although the secondary scarps located at the center of main slide was detected in 1952 photos, in 1972 they were disappeared. However, a new scarp on this slide mass was developed (Figure 3.26H). Furthermore, no changes could be detected on accumulation zone.

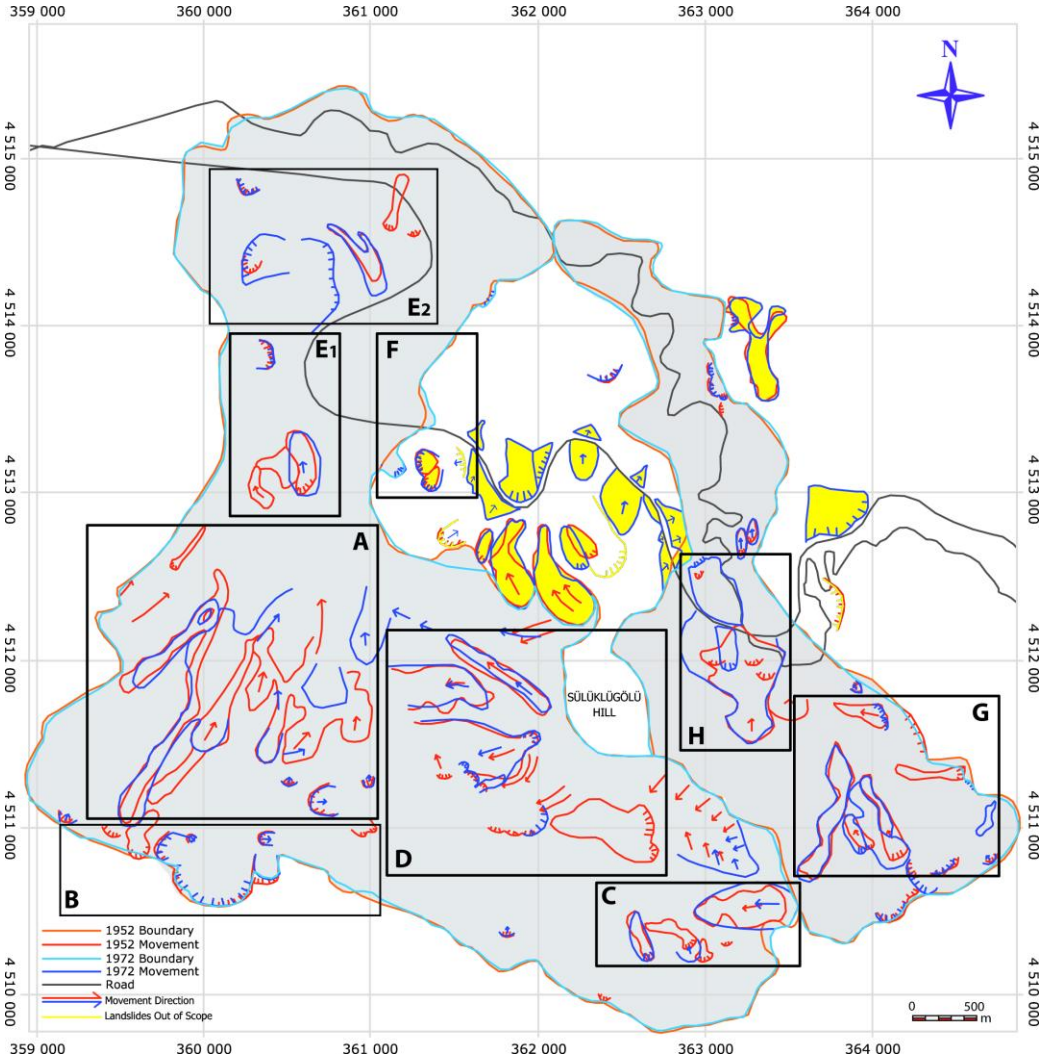

Figure 3.26. Landslide activities between 1952 and 1972 period.

3.3.2.1.3 Interpretation of the Aerial Photographs from 1984 Period

The 1984 flight was done in E-W direction at 3000m height (Figure 3.27). The first strip of flight number 3702 consists of 4 photographs that are 2959, 2958, 2957 and 2956. The second strip related to flight number 3705 contains the photographs 3009, 3010, 3011 and 3012. Total number of interpreted photographs is 8. Although the size of the photos same with the 1972 photos (23 x 23 cm), due to low flight height the scale of 1984 black and white photos were 1/15.000.

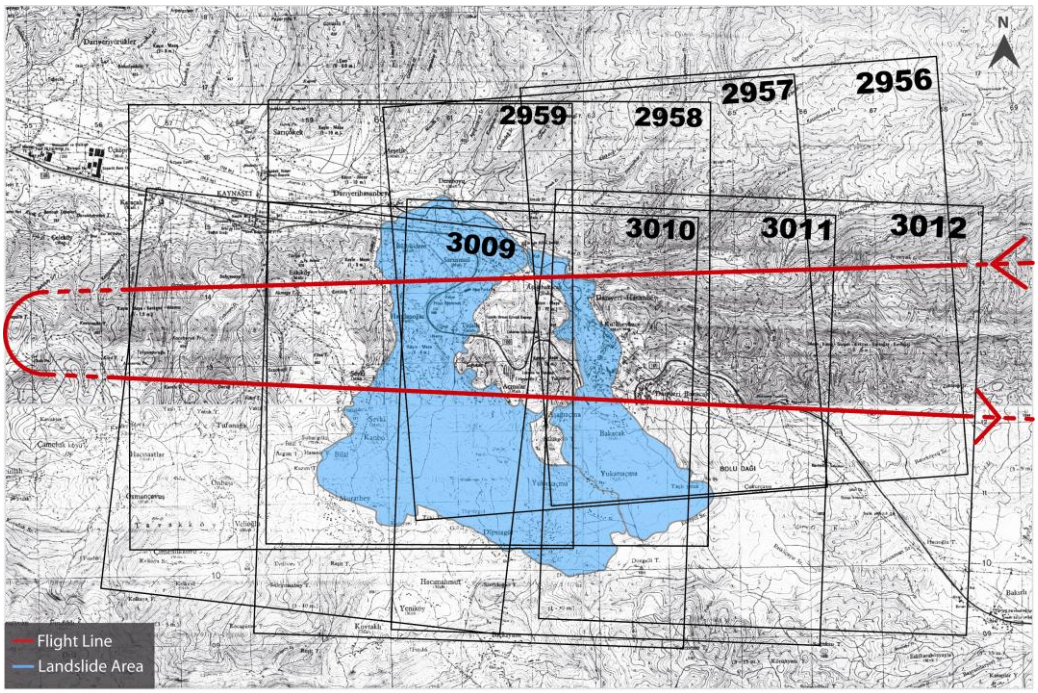

Figure 3.27. Flight plan of 1984 period on 1/25.000 scale topographic maps.

In 1984 photos it was revealed that at the western side of the Bülbülderesi landslide, progressive downslope movement of the flow was still continuing (Figure 3.28A). Besides, the flow retrogressively advanced towards the main scarp of Bülbülderesi landslide. It was remarkable that in the middle of the main body previously observed debris flows could not be distinguished in 1984 photos. The reason of this could be erosion and agricultural activities. However, the main direction of movement was realized as north-east (Figure 3.28A). The

scarp traces of minor slides at the crown of the Bülbülderesi landslide could be observed yet (Figure 3.28B). No morphological changes could be detected at the eastern side of the depletion zone. In addition, both the previously detected slides and debris flows on right flank could not be observed in 1984 photos (Figure 3.28C). Slides located at the center of the main body and at the right side of foot had decreased in size (Figure 3.28D). In 12 years period the debris flow advanced progressively at the toe of the Bülbülderesi landslide (Figure 3.28E).

Apart from some scarp traces at the main crown, most of the flows on the main body of the Bakacak landslide could be still noticed. However, in the middle of the main body previously observed debris flow could not be distinguished anymore; only its crown could be detected. In addition, it was observed that the flow located at the western side of the main body had decreased in size. Particularly, scarp traces on the main crown and at the right flank were vanished (Figure 3.28F). On the other hand, between the years 1972 and 1984 new slides had developed on the zone of accumulation. Except some parts, most of the flow at the center of main slide was vanished due to agricultural activities (Figure 3.28G). Besides, there was not any topographical change on depletion zone, except a vanished slide.

Figure 3.28. Landslide activities between 1972 and 1984 period.

3.3.2.1.4 Interpretation of the Aerial Photographs from 1994 Period

According to the flight plan of 1994 year, the flight was performed at 6050m with flight number 4442 in E-W direction (Figure 3.29). The black and white aerial photographs that cover the study area consists of 1 strip with photos of 5034, 5033 and 5032 that were 1/35.000 scale and 23 x 23 cm sized.

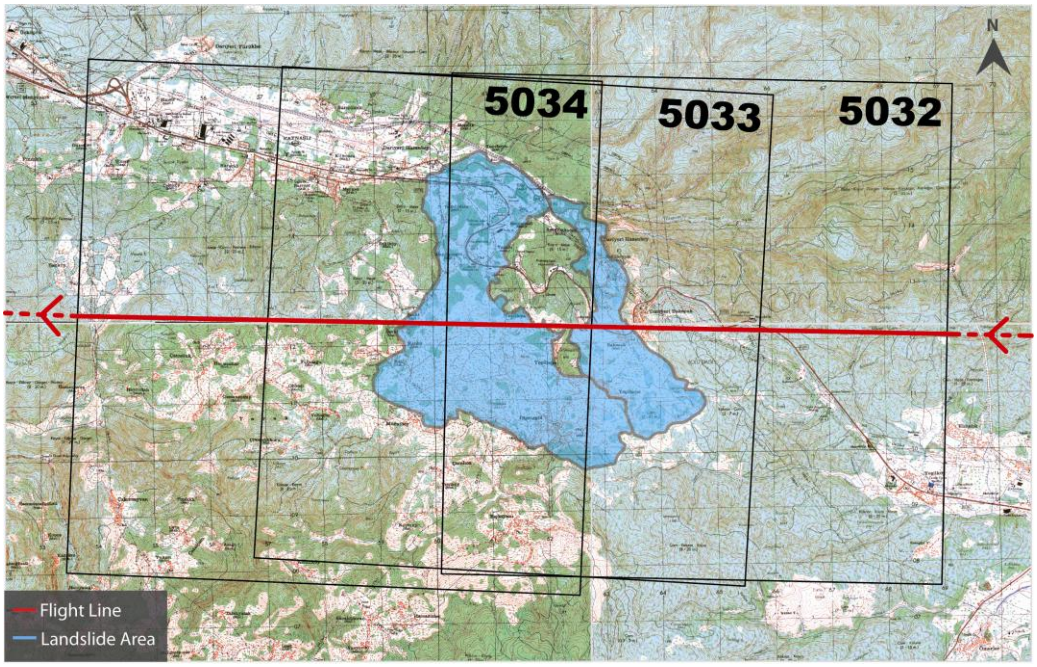

Figure 3.29. Flight plan of 1994 period on 1/25.000 scale topographic maps.

Because of the fact that no new aerial photographs were available after 1994, the last information could be gathered from 1994 photos. Also, due to 1/35.000 scale photos, details were less recognizable rather than the other photographs. At western part of the main body of the Bülbülderesi landslide, the debris flow advanced further to north-east, reactivating the main scarp of pre-1984. This fresh movement was a proof of still continuing activity. On the other hand, because of the agricultural activities and erosion the traces of downslope movement were cleared. On the main body, new slides and flows could be interpreted (Figure 3.30A). No morphological differences could be observed on the left side of head scarp. Nevertheless, most of the activities on the main body and at the right flank were completely vanished whereas there were some slides that could be still observed and may cause a disaster problem (Figure 3.30B). For instance, in Dipsizgöl Village a minor landslide could be detected both on photos and in the field check. At the toe of this slide, there were houses, a health center and a school threatened by this movement. In addition, many mass movements that could not be detected in aerial photos were observed in field

(Figure 3.31). On the other hand, it was remarkable that at the right flank, new landslides were developed (Figure 3.30C). At the western side of the accumulation zone, scarp traces of some slides could not be detected anymore. Besides, a new slide was occurred at the eastern part of toe. In 10 years period, the existing debris flow was advancing further to north-west direction at the center of accumulation zone (Figure 3.30D).

1994 photos also reveal that at the head of the Bakacak landslide no major morphological differences from 1984 could be observed, except a minor slide at the scarp. At the right flank, scarps of slides could be detected however; boundary of them could not be plotted (Figure 3.30E). Also, previously observed debris flows and scarp traces on the main body could not be distinguished in 1994 photos (Figure 3.30F). Lastly, in 10 years period a new landslide had developed on the accumulation zone whereas existing movements had become extinct (Figure 3.30G).

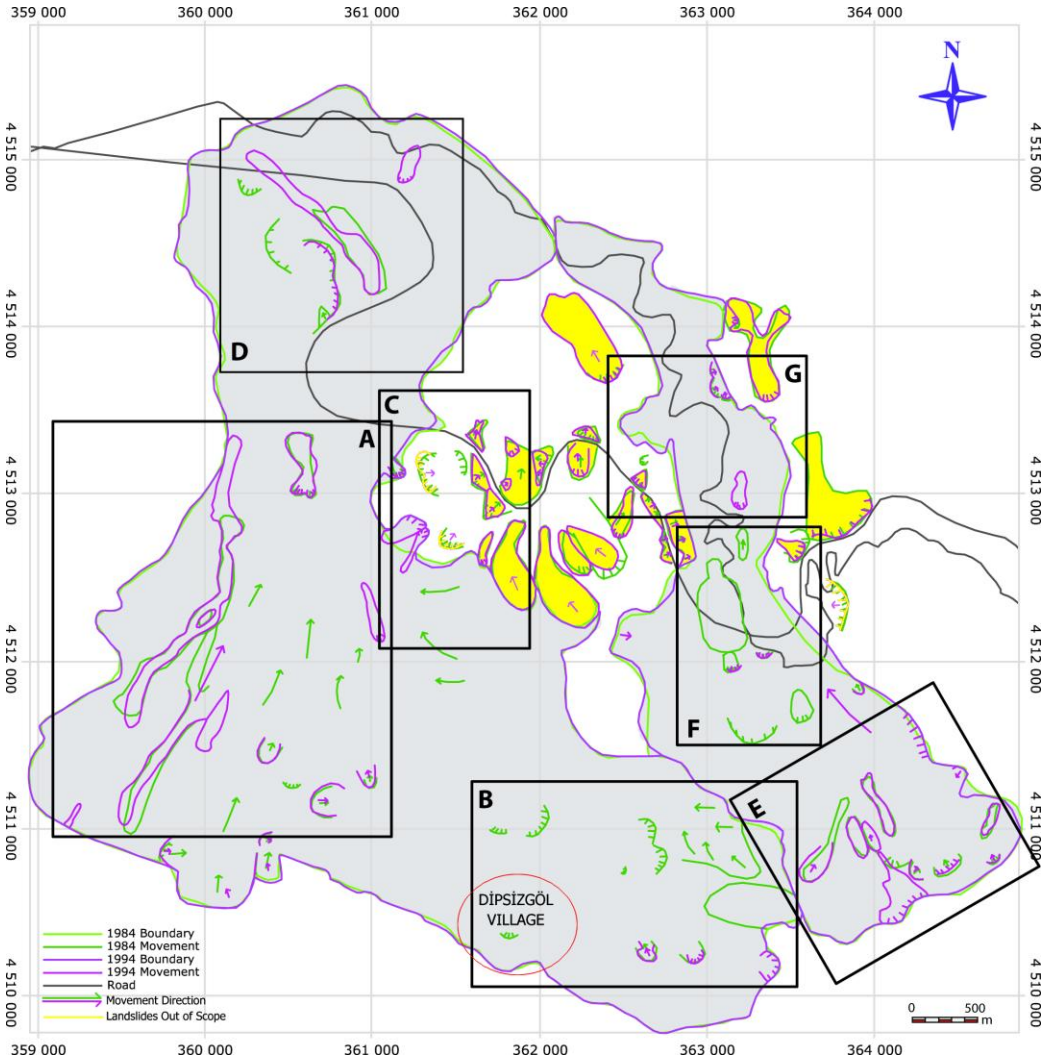

Figure 3.30. Landslide activities between 1984 and 1994 period.

When landslide activity maps of 1952 and 1994 period were compared it was seen that most of the minor slides within the main bodies were vanished due to agricultural activities and erosion. However, some minor movements of the Bülbülderesi landslide especially at the western side of the main body and at the toe could be still detected (Figure 3.32A, B). On the other hand, at the head of the Bakacak landslide common traces of minor slides corresponding to 1952 and 1994 period were observed (Figure 3.32C).

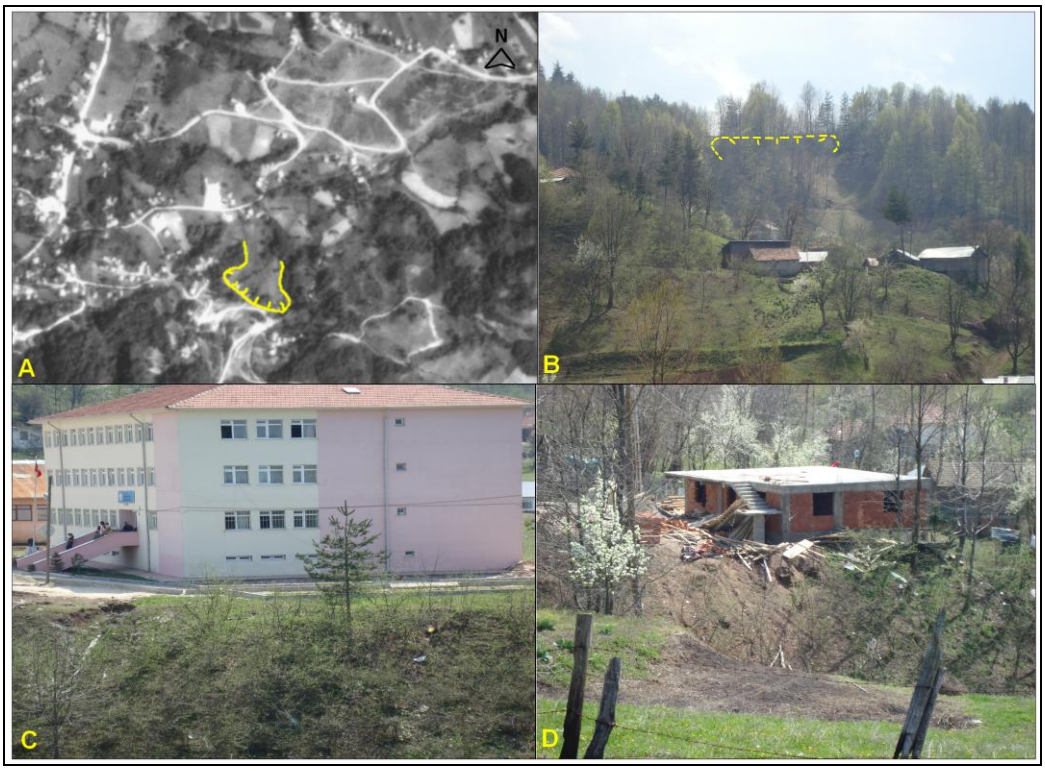

Figure 3.31. Minor slide detected on aerial photo of 1994 year (A). A view of same slide from SW (B). Minor slides observed in the school garden (C) and in the base of building construction (D).

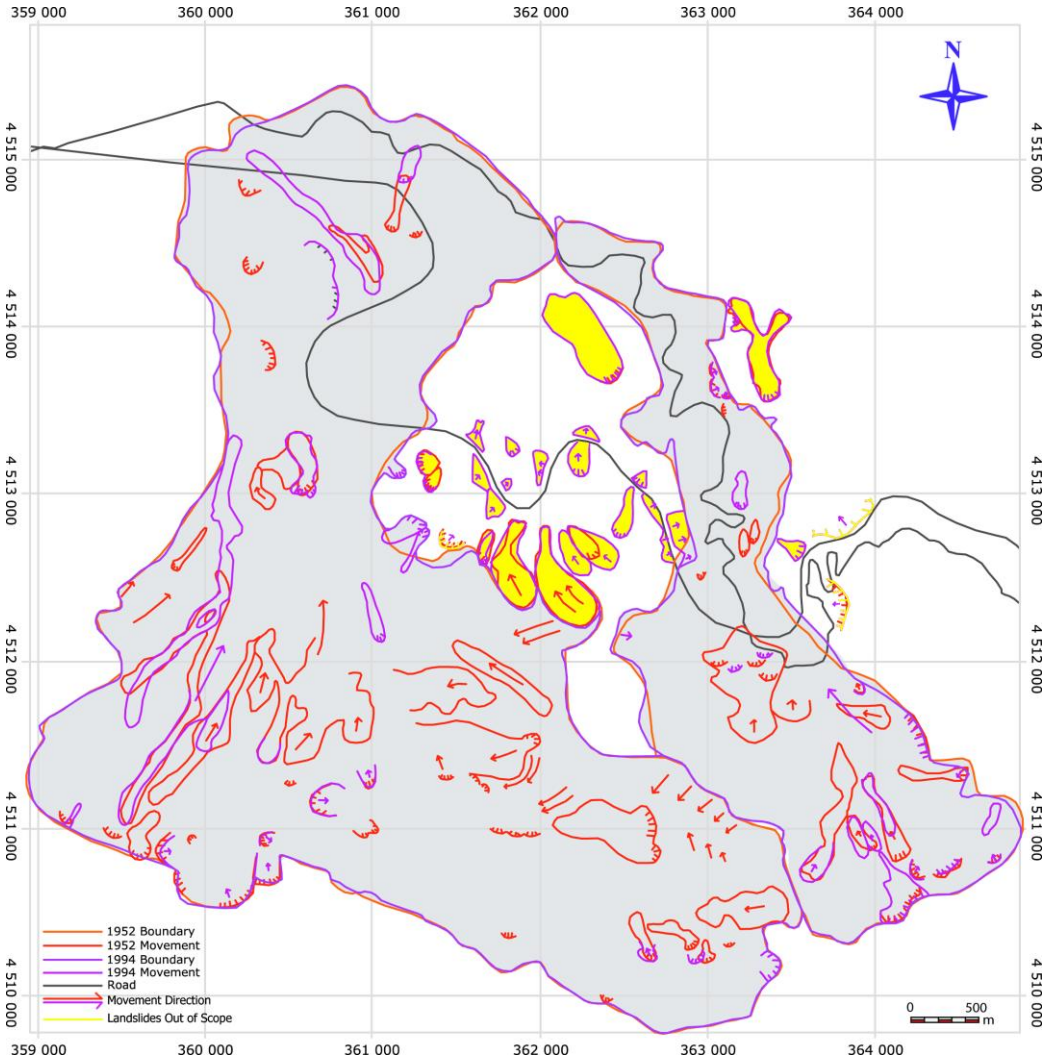

Figure 3.32. Landslide activities between 1952 and 1994 period.

CHAPTER 4

DISCUSSION AND EVALUATION

The purpose of this study was to monitor the activity of Bülbülderesi and Bakacak landslides for 42 years period by the integration of digital aerial photogrammetry and aerial photography. In accordance with the purpose of this study this chapter provides an overview of landslide monitoring step by step while discussing possible errors and their reasons.

4.1 ORTHOPHOTO MAP GENERATION

In the framework of the objectives of the thesis two datasets that are aerial photographs and topographical maps were used to produce needed data.

Scanning is the birth of the digital data and critical procedure in digital photogrammetric processing. In the stage of analogue to digital conversion of aerial photos, scanning was done by a desktop scanner. Instead of this, a photogrammetric scanner enables higher image quality and higher resolution. Scanning with photogrammetric scanners is incomparable in quality to a desktop scanner. However, desktop scanners are still the cheapest and fastest solution.

The quality of topographic maps is another significant issue in data production. Within the time, particularly 1952 and 1972 maps have been affected by atmospheric conditions such as moisture, temperature, etc., that cause deterioration in quality. Apart from coordinate mismatches, inadequate information turns the easiest georeferencing stage into a quite difficult stage. Thus, poor quality of the maps increased the RMS errors of georeferencing.

At the beginning of the thesis, the aim was to produce orthophoto maps of 4 different years by utilizing digital photogrammetric techniques and to reveal the ground displacement between these years. However, due to insufficient information in calibration reports of 1972 and 1984, even nonexistent 1952 report orthophoto map generation could not be done for these years.

Because of the fact that, the camera calibration information was available only for 1994 photos, digital photogrammetric techniques could only be applied to them in order to generate an orthophoto map. Since the orthophoto is a product that derived from other data, it is dependent of the quality of these base data. The parameters that directly affected the quality of an orthophoto are:

- The quality and resolution of source images
- Interior and relative orientation of the images
- The accuracy of digital elevation model
- The detailed information about the archive aerial photography mission (such as, camera model, camera calibration report, flight information, etc...)

The linear relation between image resolution and data accuracy is mentioned above. On the other hand, in aerial triangulation process during relative orientation the coordinates of ground control points had to be read rigorously from 1/25.000 topographical maps due to lack of GCPs' information belongs to past years. Furthermore, collecting evenly distributed GCPs is quite difficult process in densely forested areas especially northeastern side of the study area. The uncertainty of GCPs' location and the systematic errors can be reduced by collecting the coordinates of GCPs by using high precision geodetic GPS receivers in the field.

After completing aerial triangulation, stereoscopic vision was provided in order to perform software stereo plotting to obtain contour data. Because of the fact that this process was entrusted by the expert operators, it was totally

dependent on expert knowledge. Hence, DEM was created and used in orthophoto map generation which was used as a base map in further stages.

4.2 DEM GENERATION

At this point, our aim was to subtract DEMs corresponding to different epochs in order to extract the ground change between these years. To achieve this, 1/25.000 topographical maps belonging to only 1952 and 1972 could be digitized to obtain contour data due to unavailable 1984 topographical maps. Therefore, 2 DEMs were created. With the previously produced 1994 DEM, 3 DEMs of different epochs was subtracted from previously dated one that creates a surface representing the change of form over that period if there exists any. However, because of the inconsistency between the intersection parts of 1952 and 1972 sheets due to the difference in production dates, ground change detection could not be accomplished. Ideally, alternative DEMs obtained from different sources could be used in order to achieve higher accuracy. Unfortunately there were no alternative DEM sources available for this study.

4.3 AERIAL PHOTO INTERPRETATION

Having a newer sight of view, analogical interpretation of aerial photographs was performed to assess the morphological changes that occurred between 1952 and 1994. At this stage, geomorphological boundaries were identified through three-dimensional interpretation of the aerial photographs. The surface alternations were mapped onto previously produced orthophoto map to assure geometric exactness, and the possibility for quantitative comparison of the maps obtained from different epochs. Nevertheless, the manual transformation is always remaining as a large debate due to its subjectivity. Because visual interpretation dependent directly to experience of the interpreter.

CHAPTER 5

CONCLUSION

The purpose of this study is to investigate the potential use and limitations of archival aerial photographs for long-term monitoring landslide activity by means of digital aerial photogrammetry. For this purpose, Bülbülderesi and Bakacak landslides are selected as the study area. Being an economically significant area because of its proximity to both D-100 road and Anatolian Highway, Bülbülderesi and Bakacak landslides are found as appropriate study area for this thesis.

In order to generate orthophoto maps of 4 different periods, the necessary data that are topographic maps and aerial photographs were obtained. After converting the photos to digital format and georeferencing the topographic maps, to apply the digital photogrammetric techniques camera calibration parameters were needed. However, due to lack of camera calibration parameters of 1952, 1972 and 1984 period, digital photogrammetric techniques could be applied only for 1994 period. After applying block adjustment and aerial triangulation, stereo vision of 1994 photos was achieved. Then by digital photogrammetric stereoplotting contour data was generated in order to create a DEM. The DEM matrix imported on obtained stereo image enables to produce the orthophoto map of the study area.

Because of the fact that multi-temporal monitoring could not be achieved by orthophotos for 4 periods due to above reasons, it was determined to reveal the morphological changes by using DEMs. To achieve this, DEMs of 1952 and 1972 were generated by digitizing topographic maps. Due to lack of 1984 topographical maps this could not be done for 1984 period anyway. To extract

the ground change between 1952, 1972 and 1994, each DEM was subtracted from previously dated one. As a result of this, 3 differential images were obtained. However, when these images are compared with each other, it was realized that there were inconsistencies between the intersection parts of 4 sheets of 1952 and 1972 periods. The reason of this self-contradiction is the difference in production dates of the sheets. Therefore, the ground change could not be detected by the subtraction of DEMs.

Finally, aerial photo interpretation was used to investigate the activity of the Bülbülderesi and Bakacak landslides in 42 years. The information that was the size and the extent of the main boundaries and the movements inside the landslides by utilizing a mirror stereoscope was detected. After transferring visually interpreted data on to the previously produced orthophoto map which was used as a base map, landslide activity maps for each period were generated.

It is concluded that:

- Although the study area and environs were faced with 50 earthquakes, of which 2 are greater than 7 in magnitude (26.05.1957 Abant (M=7.1) and 22.07.1967 Mudurnu (M=7.2)), have been recorded from 1952 to 1994, there are no considerable variation in the position of main boundaries of Bülbülderesi and Bakacak landslides except some minor differences.
- Within the landslides there are many topographical changes explained in detail in Chapter 3 between 1952 and 1994 period. Some new minor slides have been developed; on the other hand existing slides could not be detected anymore due to agricultural activities and erosion.
- Bülbülderesi and Bakacak landslides extend through Ankara-İstanbul E5 highway have jeopardized the stability of the highway at various locations. Although, the slides were detected and transferred on to the base map, they were not taken into

consideration for this study. These interpretations should be considered as the first attempts for more detailed analysis.

- Based on the profile from toe to crest of the Bülbülderesi landslide, the approximate length was measured as 4773m whereas the approximate width was about 2614m. The extent was calculated as ~12km^2 having an approximate slope gradient between 10-15° with local variations. East side of the landslide is always elevated more than that of its west side.
- The approximate length of Bakacak landslide was 4420m and the approximate width was 832m from toe to crest with an area of ~4km^2 and with an approximate slope angle 9-14°.
- According to the information gathered from performed studies it is concluded that Bakacak and Bülbülderesi landslides are not active but there exists minor slope instabilities on the previously slided mass of these landslides.

REFERENCES

Abdülselamoğlu, S., 1959, Almacıkdağı ile Mudurnu ve Göynük civarının jeolojisi, İstanbul Üniversitesi, Fen Fakültesi Monografileri, 14.

Adams, J. C. and Chandler, J. H., 2002, Evaluation of Lidar and Medium Scale Photogrammetry for Detecting Soft-Cliff Coastal Change, Photogrammetric Record 17 (99): pp. 405-418

Ager, G., Marsh, S., Hobbs, P., Chiles, R., Haynes, M., Thurston, N. and Pride, R., 2004, Towards Automated Monitoring of Ground Instability Along Pipelines, Proceedings of the Institute of Civil Engineers, Geopipe 2004 Conference, London, UK.

Aksu, T.S., 2002, Gümüşova (Düzce)-Gerede (Bolu) arası Asarsu vadisinin mühendislik jeolojisi ve depremsellik açısından incelenmesi, Yüksek Lisans Tezi, İstanbul Teknik Üniversitesi Fen Bilimleri Enstitüsü, 106 s.

Aktimur, T., Algan, Ü., Ateş, Ş., Oral, A., Ünsal, Y., Karatosun, H., Öztürk, V. and Sönmez, M., 1983, Bolu ve yakın çevresinin yerbilimleri sorunları ve muhtemel çözümleri, MTA Rap No:7387 (unpublished)

Akyüz, H.S., Barka, A., Altunel, E., Hartleb, R. and Sunal, G., 2000, Field observations and slip distributions of the November 12, 1999 Düzce earthquake (M=7.1), Bolu – Turkey. In 1999 Izmit and Düzce Earthquakes: preliminary results, Barka, A., Kozacı, Ö., Akyüz, S. and Altunel, E. İstanbul University Press. Istanbul. 63-70.

Ambraseys, N.N., 1970, Some characteristic features of the North Anatolian Fault Zone, Tectonophysics, 9, 143-165.

Astaldi, 1990, Geological report: Preliminary design Anatolian Motorway Gümüşova-Gerede stretch No: 2, Report number 2014.

Aydan, Ö., Ulusay, R., Kumsar, H. and Tuncay, E., 2000, Site investigation and engineering evaluation of the Düzce-Bolu earthquake of November 12, 1999, Turkish Earthquake Foundation, TDV/DR 09-51, 220p.

Aydan, Ö. and Dalgıç, S., 1998, Prediction of deformation behaviour of 3-lanes Bolu Tunnels through squeezing rocks of North Anatolian Fault Zone (NAFZ). Regional Symp on Sedimentary Rock Engineering. Taipei, Taiwan, 1998, 228-233

Aydın, M., Serdar., S., Şahintürk, Ö., Yazman, M., Çokuğraş, R.,Demir, O. and Özçelik, Y., 1987, Çamdağ (Sakarya) – Sünnicedağ (Bolu) yöresinin jeolojisi, TJK bülteni, 30, 1-14.

Bajracharya, B., and Bajracharya S. R., 2006, Landslide Mapping of The Everest Region Using High Resolution Satellite Images and 3D Visualization, International Conference on Space Technology and Geo Informatics

Barka, A., and Erdik, M., 1993, Active Faults of Gümüşova-Gerede Highway, Bolu Mountain, Astaldi report, 25p.

Batum, İ., 1968, 1/25.000 ölçekli Adapazarı G26-b3 paftasının Jeolojisi, MTA Rap No:4778 (unpublished)

Blumenthal, M., 1948, Bolu civarı ile Aşağı Kızılırmak mecrası arasındaki Kuzey Anadolu silsilelerinin jeolojisi, MTA Yayınları, Seri B, No:13, 265p.

Bovenga, F., Nutricato, R., Refice A., and Wasowki, J., 2006, Application of Multi-temporal Differential Interferometry to Slope Instability Detection in Urban/Peri-urban Areas, Engineering Geology 88 pp. 218–239

Burrough, P. A. and McDonnel, R. A., 1998, Principles of Geographical Information Systems, Oxford University Press, Oxford: 333 pp.

Canik, B., 1980, Bolu sıcak su kaynaklarının hidrojeolojisi, Selçuk Üniversitesi Fen Fakültesi Yayınları, 1, 74 p.

Cardenal, J., Delgado J., Mata E., González A., and Olague, I., 2006, Use of historical flight for landslide monitoring, 7th International Symposium on Spatial Accuracy Assessment in Natural Resources and Environmental Sciences.

Cencetti, C., Conversini, P., Radicioni, F., Seli S. and Tacconi P.,2000, The Evolution of Montebestia Landslide (Umbria, Central Italy). Site Investigations,In-Situ Tests and GPS Monitoring, Phys. Chem. Earth (B), Vol. 25. No. 9. pp. 799-808

Cerit, O., 1983, Mengen (Bolu NE) yöresinin jeolojik incelenmesi, Yüksek lisans tezi, Hacettepe Ü., 160 s.

Cerit, O., 1990, Bolu Masifinin jeolojik ve tektonik incelemesi, Doktora Tezi, Hacettepe Ü., 217p.

Chandler, J. H., 1999, Effective Application of Automated Digital Photogrammetry for Geomorphological Research, Earth Surface Processes and Landforms 24 (1): pp. 51-63.

Cheng, H. H., 2000, Photogrammetric Digital Data Processing of Tsau-Lin Big Landslide, Proceedings of the 21st Asian Conference on Remote Sensing, Taipei, Taiwan.

Clarke, T.A., and Fryer, J.F., 1998, The development of camera calibration methods and models, Photogrammetric Record, 16(91): pp 51-66.

Colesanti C. and Wasowski J., 2006, Investigating landslides with space-borne Synthetic Aperture Radar (SAR) Interferometry, Engineering Geology 88 pp. 173–199

Corominas J., Moya J., Lloret A., Gili J.A., Angeli M.G., Pasuto A., 2000, Measurement of landslide displacements using a wire extensometer. Eng Geol 55:149–166

Dalgıç, S., 1994a, Anadolu Otoyolu Bolu Dağı geçişinin mühendislik jeolojisi, Doktora Tezi, İstanbul Üniversitesi, Fen bilimleri Enstitüsü, 213p. (unpublished)

Dalgıç, S., 1994b, Anadolu Otoyolu Bolu Dağı geçişinin mühendislik jeolojisi, Türkiye Jeoloji Kurultayı Bülteni, 9, 393-397.

Dalgıç, S., 1997, Distribution of lithological and structural features along Bolu Tunnel, Anatolian Motorway, Geological Bulletin of Turkey, 40-2,39-48.

Dalgıç, S.,1998a, Slope stability problems of the weak rocks in the Asarsuyu pass of the Anatolian Motorway. Bull. Eng. Geol. Env., 57, 199-206.

Dalgıç S., 1998b, Selection of crushed rock quarries for the construction of the Anatolian Motorway ,Environmental & Engineering Geoscience ,4: (4) 511-518

Dalgıç, S. and Gözübol, A.M., 1995, Bolu otoyol tünelinde stabilite problemleri. Geosound, 27, 73-80.

Dalgıç, S., Şimşek, O. and Gözübol, A.M., 1995 Anadolu otoyolu Bolu Yumrukaya geçişinde heyelanların etkisi, İkinci Ulusal heyelan Sempozyumu, Adapazarı, 163-170.

Dalgıç, S. and Şimşek O., 2002, Settlement predictions in the Anatolian Motorway, Turkey, Engineering Geology, 67 (1-2): 185-199.

Demirtaş, R., 1993, İğneciler (Bolu)-Dokurcun (Adapazarı) arasında Kuzey Anadolu fay zonunun neotektonik özellikleri ve depremselliği, Yüksek Lisans Tezi, Ankara Üniversitesi Fen Bilimleri Enstitüsü, 83 s.

Demirtaş, R., 2000, Kuzey Anadolu Fay Zonu'nun Abant-Gerede arasinda kalan bölümünün neotektonik özellikleri ve paleosismisitesi, Doktora Tezi, Ankara Üniversitesi Fen Bilimleri Enstitüsü, 211 s.

Erendil, M., Aksay, S., Kuşçu, İ., Oral, A., Tunay, G. and Temren, A., 1991, Bolu masifi ve çevresinin jeolojisi, MTA Rap No:9425 (unpublished)

Fernández T., Delgado J., Cardenal J., Irigaray C., El Hamdouni R., and Chacón J., 2006, Use of historical flight for landslide monitoring, 7th International Symposium on Spatial Accuracy Assessment in Natural Resources and Environmental Sciences.

Franklin, J. A., 1984, Slope Instrumentation and Monitoring, In: Brunsden, D. and Prior, D. B. (eds.), Slope Instability, John Wiley and Sons, Chichester: pp. 143-169.

Gallousi C., Koukouvelas, I. K., 2007, Quantifying geomorphic evolution of earthquake-triggered landslides and their relation to active normal faults. An example from the Gulf of Corinth, Greece, Tectonophysics 440 pp. 85–104

Gedik, A., ve Alkaş, İ, 1996, Bolu yöresinin Jeolojisi ve karbondioksit olanakları, MTA rap No: 10147. (unpublished)

Gili, J. A., Corominas, J. and Rius, J., 2000, Using Global Positioning System Techniques in Landslide Monitoring. Engineering Geology 55 (3): pp. 167-192.

Görmüş, S., 1980, Yığılca (Bolu NW) yöresinin jeolojik incelemesi, Doktora Tezi, Hacettepe Üniversitesi. 210s.

Görmüş, S., 1982a, Yığılca (Bolu KB) yöresinin stratigrafisi, H.Ü. Yerbilimleri, 9, 91-110.

Görmüş, S., 1982b, Yığılca (Bolu KB) yöresinin tektoniği ve jeolojik evrimi, H.Ü. Yerbilimleri, 9, 133-140.

Gözübol, A.M., 1978, Mudurnu-Dokurcun-Abant (Bolu ili) alanının jeoloji incelemesi ve Kuzey Anadolu yarılımının yapısal özellikleri, Doktora tezi, İstanbul Üniversitesi Fen Fakültesi Tatbiki Jeoloji Kürsüsü.

Güler, B., 1999, Bolu Dağı Bakacak (Bolu) yöresi jipslerinin jeolojik incelemesi, Yüksek Lisans Tezi, Hacettepe Ü., 46 s.

Gürbüz, M., Koç, N., Hamzaçebi, G., 2005, Jeofiziksel Yaklaşımlarla Heyelan Yapısının Araştırılması, Deprem Sempozyumu Kocaeli (poster sunum)

Hervás, J., Barredo, J. I., Rosin, P. L., Pasuto, A., Mantovani, F. and Silvano, S., 2003, Monitoring Landslides from Optical Remotely Sensed Imagery: The Case History of Tessina Landslide, Italy. Geomorphology 54 (1-2): 63-75.

Hitchcock, C.S., Altunel, E., Barka, A., Bachhuber, J., Lettis, W., Kozaci, O., Helms, J., and Lindvall, S., 2003, Timing of Late Holocene Earthquakes on the Eastern Düzce Fault and Implications for Slip Transfer between the Southern and Northern Strands of the North Anatolian Fault System, Bolu, Turkey: Turkish Journal of Earth Sciences, v. 12, Issue 1, pp. 119-136.

Işın, Z.S., 1999, D-100 (E-5) Karayolu, Bolu Dağı geçişi, Kaynaşlı – Elmalık arasının mühendislik jeolojisi ve Taşaltı Heyelan Bölgesinin jeoteknik değerlendirilmesi, Yüksek Lisans Tezi. İ.T.Ü., 145s.

Karabörk H., Yıldız F. ve Çoşkun E., 2004, Object recognition for interior orientation in digital photogrammetry, Proceedings of the 20th Congress of

International Society for Photogrammetry and RemoteSensing, 12-23 July, İstanbul, Turkey.

Karaçam, A., 2005, Gökçesu civarı (Bolu) birimlerinin rezervuar jeolojisi özelliklerinin incelenmesi, Yüksek Lisans Tezi, Ankara Üniversitesi Fen Bilimleri Enstitüsü, 97 s.

Karsli, F., Yalcin, A., Atasoy, M., Demir, O., Reis, S., Ayhan, E., 2004, Landslide Assessment by using Digital Photogrammetric Techniques,20th ISPRS Congress, 12-23 July, 2004, Turkey.

Kaya, O., 1982, Ereğli, Yığılca, Bolu Kuzey, Mengen alanlarının stratigrafisi ve yapı özellikleri. TPAO Rap No: 1639. (unpublished)

Kaya, O. and Dizer, A., 1981-1982 a, Mengen (Bolu) Eosen kömür havzasının stratigrafisi. MTA dergisi 97/98, 123 – 133.

Kaya, O. and Dizer, A., 1981-1982 b, Bolu Kuzeyi Üst Kretase ve paleojen kayarının stratigrafisi ve yapısı. MTA dergisi, 97/98, 57-77.

Kaya, O., Dizer, A., Tansel, İ. and Özer, S., 1986, Yığılca (Bolu) alanı üst Kretase ve Paleojeninin stratigrafisi, MTA derg., 107, 13-31.

Kazak, B., 2004, Bolu ovası güneydoğu kesminin jeolojisi ve neotektoniği, Yüksek Lisans Tezi, Cumhuriyet Üniversitesi Fen Bilimleri Enstitüsü, 85 s.

Ketin, İ, 1955, Akçakoca-Düzce bölgesinin jeolojik lövesi hakkında memuar, MTA Rap No:2277 (unpublished)

Ketin, İ., 1967, Bolu – Gerede – Mengen ve Yığılca bölgesindeki Paleozoyik oluşuklara ait jeolojik rapor, TPAO Arama Grubu Rap No: 379. (unpublished)

Ketin, İ., 1969, Kuzey Anadolu Fayı hakkında. MTA Enstitusü Dergisi, 72, 1-27.

Konecny, G., 1985, The International Society for Photogrammetry and Remote Sensing - 75 Years Old or 75 Years Young, Photogrammetric Engineering and Remote Sensing 51 (7): pp. 919-933.

Koral, H., Dalgıç, S. and Gözübol, 1994, Bolu masifi gabroyik kayalarında mikrofabrik çalışma. Türkiye Jeoloji Kurultayı Bülteni, 9, 183-187.

Lane, S. N., Richards, K. S. and Chandler, J. H., 1993, Developments in Photogrammetry; the Geomorphological Potential, Progress in Physical Geography 17: pp. 306-328.

Lane, S. N., Chandler, J. H. and Richards, K. S., 1994, Developments in Monitoring and Modeling Small Scale River Bed Topography, Earth Surface Processes and Landforms 19: pp. 349-368.

Malet, J. P., Maquaire, O., Calais, E., 2002, The use of Global Positioning System for the continuous monitoring of landslides. Application to the Super-Sauze earthflow (Alpes-de-Haute-Provence, France).Geomorphology, 43, 33-54.

Mayuzumi, N., Ogawa S., 2006, Diastrophism Evaluation of Niigata Chuetsu Earthquake by Aerial Photography**,** 27th Asian Conference on Remote Sensing (ACRS 2009) Ulaanbaatar, Mongolia

Mikhail, E.M., Bethel, J.S., and McGlone, J.C., 2001, Introduction to Modern Photogrammetry. John Wiley & Sons, New York, pp. 113-115

Mora, P., Baldi P., Casula G., Fabris M., Ghirotti M., Mazzini E., and Pesci A., 2003, Global Positioning Systems and digital photogrammetry for the

monitoring of mass movements: application to the Ca' di Malta landslide (northern Apennines, Italy), Engineering Geology 68 pp. 103–121

MTA, 2002, 1/500.000 ölçekli Türkiye Jeoloji Haritası Zonguldak Paftası, MTA Yayınları

Neugebauer, J., 1994, Closing-up structures, alternatives to pull-apart basins; the effect of bends in the North Anatolian Fault, Turkey, Terra Nova, 6, 359-365.

Neugebauer, J., 1995, Structures and kinematics of the North Anatolian Fault zone, Adapazarı-Bolu region, northwest Turkey. Tectonophysics, 243, 119-134.

Neugebauer, J., Löflerr, M., Berckhemer, H., Yatman, A., 1997, Seismic observations at an overstep of the western North Anatolian Fault (Abant-Spanca region, Turkey). Geol Rundsch, 86, 93-102.

Nurlu, M., 1993, Kuzey Anadolu Fay Zonunda, (Bolu-Sapanca gölü arası) etken olan gerilimlerin fay analizleri ve uydu görüntüleri yardımı ile saptanması. 46. Türkiye Jeoloji Kurultayı Bildiri özleri. p. 121.

Okay, N., 2005, The Risk Profile and Disaster Management System of Turkey, WBI-Natural Disaster Risk Management Program-Final Project.

Orkan, N.İ., Aktimur, H., Sungur, G. and Işıklar, İ .S., 1977, Ankara-İstanbul Otoyolu güzergahı Bolu Dağı jeoloji incelemesi, MTA Rap No:2277 (unpublished)

Özben, M. 2003, Bolu dağı tüneli mühendislik jeolojisi ve kazı sırasında karşılaşılan jeolojik ve jeoteknik sorunların tünel kazı ve destek sistemi üzerindeki etkileri, Doktora tezi, Çukurova Üniversitesi Fen Bilimleri Enstitüsü, 151 s.

Özden S., Tatar O., Mesci, B. L., Koçbulut F., Tutkun S. Z., Doğan B., Tüvar O., 2000, 12 Kasım 1999 Düzce Depremi ve Bölgesel Tektonik Anlamı, Türkiye Jeoloji Bülteni, Cilt 43, Sayı 2, 69s.

Özmen, B., 2000, Düzce-Bolu Bölgesi'nin Jeolojisi, Diri Fayları ve Hasar Yapan Depremleri s:1-14, 12 Kasım 1999 Düzce Depremi Raporu, Bayındırlık ve İskan Bakanlığı Afet İşleri Genel Müdürlüğü, Deprem Araştırma Dairesi, Ankara, 14s.

Öztürk A., İnan, S. and Tutkun, Z., 1984, Abant-Yeniçağa (Bolu) yöresinin tektoniği, Cumhuriyet Üniversitesi, Yerbilimleri, 1, 1-18.

Pamuksuz, Z., 2007, Köprübaşı barajı (Mengen-Bolu) ve hes inşaatı mühendislik jeolojisi incelemesi, Yüksek Lisans Tezi, Selçuk Üniversitesi Fen Bilimleri Enstitüsü, 163 s.

Pucci, S., Pantosti, D., Barchi, M.R., and Palyvos, N., 2007, A complex seismogenic shear zone: The Düzce segment of North Anatolian Fault (Turkey),Earth and Planetary Science Letters 262, 185–203

Scheuren, J. M., Le Polain De Waroux, O., Below, R., Guha-Sapir, D., and Ponserre, S., 2008, Annual Disaster Statistical Review The Numbers and Trends 2007, Center for Research on the Epidemiology of Disasters (CRED), Brussels.

Serdar, H. and Demir, C., 1983, Mengen-Bolu-Abant dolayı jeolojisi ve petrol olanakları. TPAO raporu. (unpublished).

Simard, P. G., 1997, Accuracy of Digital Orthophotos, M.S. Thesis, The University of New Brunswick, Canada, pp.133.

Smith, W. K., 1996, Photogrammetric Determination of Slope Movements on the Slumgullion Landslide, In: Varnes, D. J. and Savage, W. Z. (eds.) The

Slumgullion Earth Flow: A Large-Scale Natural Laboratory, U.S. Geological Survey Bulletin 2130. U.S. Government Printing Office, Washington.

Sözen, A., Erbayar, M., Çamaşırcıoğlu, A. ve Çeltek, N., 1996, Düzce (Bolu) - Devrek (Zonguldak) yöresinin genel jeokimya raporu, MTA Rap No: 9922. (unpublished).

Sucuoğlu, H.,Bakır, S., Tankut, T., Erberik, A., Gülkan, P., Özcebe, G., Gür, T., Yılmaz, Ç., Ersoy, U., Yılmaz, T. and Akkar, S., 2000, Marmara ve Düzce depremleri mühendislik raporu, Deprem Mühendisliği Araştırma Merkezi, 174 p.

Süzen, M. L., 2002, Data driven landslide hazard assessment using geographical information systems and remote sensing, M.E.T.U. PhD Thesis, Unpublished, 196 pp. http://www.metu.edu.tr/~suzen

Süzen, M.L. and Doyuran, V., 2004a, Data driven bivariate landslide susceptibility assessment using geographical information systems: a method and application to Asarsuyu catchment, Turkey, Engineering Geololgy, vol 71/3-4 pp. 303-321

Süzen, M.L. and Doyuran, V., 2004b, A comparison of the GIS based landslide susceptibility assessment methods multivariate versus bivariate, Environmental Geololgy, vol 45/5, 665/679

Şaroğlu, F., Herece, E., Sarıaslan, M., Emre, Ö., 1995, Yeniçağa-Gerede-Eskipazar arasının jeolojisi ve Kuzey Anadolu Fayı'nın genel özellikleri. MTA Rap No: 9873 (unpublished)

Şengör, A.M.C. and Canitez, N., 1982, The North Anatolian Fault. In: Alpine Mediterranean Geodynamics, Berekhemer, H. and Hsu, K. (eds). Deuticke, Vienna, 205-216.

Şengör, A.M.C., Tüysüz, O., İmren, C., Sakınç, M., Eyidoğan, E., Görür, N., Le Pichon, X. and Rangin, C., 2005, The North Anatolian Fault: A new look, Annu. Rev. Earth Planet. Sci., 33, 1-75.

Şentürk, C.H., 1999, Bolu Dağı tünelinin mühendislik jeolojisi ve jeoteknik özelliklerinin destek sistemine etkisi, Yüksek Lisans Tezi, Kocaeli Üniversitesi Fen Bilimleri Enstitüsü, 186 s.

Şimşek, O. and Dalgıç, S., 1997, Consolidation properties of the clays at Düzce plain and their relationship with geological evaluation, Geological Buletin of Turkey, 40(2), 29-38.

Taymaz, T., 2000, Seismotectonics of Marmara Region: Source characteristics of 1999 Gölcük – Sapanca – Düzce Earthquakes. In 1999 Izmit and Düzce Earthquakes: preliminary results, Barka, A., Kozacı, Ö., Akyüz, S. and Altunel, E. Istanbul University Press. Istanbul. 79-97

Tralli, D.M., Blom, R.G., Zlotnicki V., Donnellan, A., Evans, D. L., 2005, Satellite remote sensing of earthquake, volcano, flood, landslide and coastal inundation hazards, ISPRS Journal of Photogrammetry and Remote Sensing 59 (4): 185-198

TMMOB Jeoloji Mühendisleri Odası, 2006, 20. Dönem Çalışma Raporu 2004-2006, 500–534.

Tokay, M., 1973, Kuzey Anadolu Fay Zonunun Gerede ile Ilgaz arasındaki kısmında jeolojik gözlemler. Kuzey Anadolu Fayı ve deprem kuşağı sempozyumu. 12-29.

Unterberger, W. and Brandl, J., 2000, The effect of recent earthquake in Turkey on the Bolu Tunnels, Felsbau, 18-2, 50-54.

Ustaömer, P.A. and Rogers, G., 1999, The Bolu Massif: remnant of a Pre-Early Ordovicien active margin in the west Pontides, northern Turkey. Geological Magazine, 136, 5, 579-592.

Uysallı, H., 1959, Bolu - Merkeşler bölgesinin jeolojisi ve linyit imkanları. MTA Enstitusü dergisi sayı 52, 107 p.

Varnes D. J., 1978, Slope movement types and processes. In: Schuster R. L. & Krizek R. J. Ed., Landslides, analysis and control. Transportation Research Board Special Rep. No. 176, National Research Council, Washington, pp 11–33

Weibel, R. and Heller, M., 1991, Digital Terrain Modeling. In: Maguire, D. J., Goodchild, M. F. and Rhind, W. D. (eds.) Geographical Information Systems: Principles and Applications. Longman, London: pp. 269-297.

Wolf, P. R. and Dewitt, B. A., 2000, Elements of Photogrammetry with Applications in GIS. McGraw-Hill, Boston: 608 pp.

Yalçın, H. and Cerit, O., 1991, Bolu masifi örtü kayaçlarında diyajenetik ve çok düşük dereceli metamorfik kil minerallerinin mineralojisi ve jeokimyası. C.Ü. Müh. Fak. Der. Seri A. Yerbilimler C.8,1.

Yalçınkaya, M. and Bayrak, T., 2001, Developing a dynamic deformation model for landslides, Fourth Turkish-German Joint Geodetic Days, Berlin: pp. 583-590.

Yeşilnacar, E. and Süzen, M.L., 2006, A land-cover classification for landslide susceptibilty mapping by using feature components, International Journal of Remote Sensing, Vol:27, No:2, 253-275

Yılmaz, Y., Gözübol A.M., Tüysüz, O. and Yiğitbaş., 1981, Abant (Bolu)-Dokurcun (Sakarya) arasında Kuzey Anadolu Fay Zonunun kuzey ve güneyinde kalan tektonik birliklerin evrimi, İ.Ü.Yerbilimleri der., 2, 231-261.

Yugsi, F., Eisenbeiss, H.., Remondino, F., Winkler, W., 2006, Multi-temporal monitoring of landslides in archaeological mountainous environments using optical imagery: The case of El Tambo, Ecuador, 173-178

ONLINE REFERENCES

URL1: EMDAT (Emergency Events Database), http://www.emdat.be/Database/AdvanceSearch/emdat_chooser.php, (visited on 01.03.2009)

URL2: General Directorate of Disaster Affairs, http://www.deprem.gov.tr/linkhart.htm, (visited on 12.01.2009)

URL3: Sayısal Grafik, http://www.sayisalgrafik.com.tr/deprem/tr_frames.htm, (visited on 11.03.2009)

URL4: General Command of Mapping, http://www.hgk.mil.tr/urunler/haritalar/yurticiuretim/topografik/topotek25.html